Microwave Plasma CVD Grown Single Crystal Diamonds – A Review

Awadesh Kumar Mallik[*]

CSIR – Central Glass & Ceramics Research Institute, 196 Raja S C Mullick Road, Kolkata, 700032, West Bengal, India

Abstract: Diamond offers a range of unique properties, including wide band of optical transmission, highest thermal conductivity, stiffness, wear resistance and superior electronic properties. Such high-end properties are not found in any other material, so theoretically it can be used in many technological applications. But the shortcoming has been the synthesis of the diamond material in the laboratory for any meaningful use. Although microwave plasma chemical vapour deposited (MPCVD) has been in practice since 1980s for the diamond growth but it is in the past 7-8 years that its potential has been realised by the industry due to capability of MPCVD to deposit diamond, pure and fast, for commercial uses. There are many CVD techniques for growing diamond but among them MPCVD can only make single crystal diamond (SCD) effectively. SCD grown by MPCVD is also superior to other forms of diamond produced in the laboratory. For example, SCD is necessary for the best electronic properties - often outperforming the polycrystalline diamond (PCD), the high pressure high temperature (HPHT) diamond and the natural diamond. In many applications the short lateral dimensions of the lab-grown diamond available is a substantial limitation. Polycrystalline CVD diamond layers grown by hot filament CVD solved this problem of large area growth, but the presence of grain boundaries are not appropriate for many uses. On the other hand, there is still limitation in the area over which SCDs are grown by MPCVD, only upto 10-15 mm lateral sizes could have been achieved so far, while there are recipes which rapidly grow several mm thick bulk SCDs. This lateral size limitation of SCDs is primarily because of the small seed substrate dimension. Although natural and HPHT diamonds may not be suitable for the intended application, still they are routinely used as substrates on which SCD is deposited. But the problem lies in the availability of large area natural SCD seeds which are extremely rare and expensive. Moreover, large diamond substrate plates suitable for CVD diamond growth have not been demonstrated by HPHT because of the associated high economic risk in their fabrication and use. Other than lateral dimension, purity of SCD is also very important for technological use. Natural diamond is often strained and defective, and this causes twins and other problems in the CVD overgrowth or fracture during synthesis. In addition, dislocations which are prevalent in the natural diamond substrate are replicated in the CVD layer, also degrading its electronic properties. HPHT synthetic diamond is also limited in size, and generally is of poorer quality in the larger stones, with inclusions being a major problem.

There will be much research interest in the next 10 years for the MPCVD growth of SCD. Purer and bigger SCDs will be tried to grow with faster and reproducible MPCVD recipes. Here the MPCVD growth of SCD is being reviewed keeping in mind its huge technological significance in the next decades or so. Discoveries of the commercial productions of silicon, steel, cement different materials have built modern societies but higher scales will be achieved with the advent of lab-grown diamond.

1. INTRODUCTION

Scopus search, with "single crystal diamond" in the title, abstract and keywords of the articles, published during 1980-1989, came back with only 277 results. This was because during 1980s researchers were busy in understanding the metastable CVD growth process of diamond (other synthetic diamond was popularly called HPHT diamond). Once CVD became an established technology for growing diamond in the laboratory, the concentration shifted to produce diamond for industrial uses during 1990s. Homoepitaxy [1] was already in place prior to the advent of heteroepitaxy [2-12]. For the periods 1990-94 (505 papers) and 1995-99 (884 papers) similar Scopus search showed much more numbers of scientific articles. But the research in this field picked up only from the year 2003 (as shown in Figure **1**). From the very beginning of synthetic diamond research (1950s), various groups had been trying to synthesise diamond on top of diamond seed itself. But homoepitaxy substrates were rather small in size (<0.5mm) for any practical engineering

[*]196 Raja S C Mullick Road, Kolkata, 700032, West Bengal, India; Tel: +91 33 24733476; Fax: +91 33 24730957; E-mail: amallik@cgcri.res.in
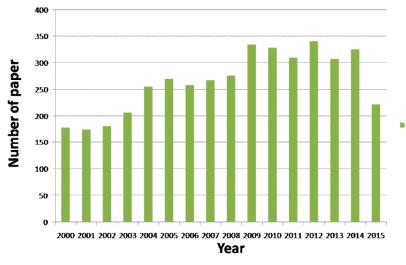
Figure 1: Publication statistics of "single crystal diamond" research.

application. So there came the need of diamond heteroepitaxy [13-16], because large substrate sizes of silicon, c-BN, β-SiC etc were already available. But the hetero-epitaxially grown diamond grains were not large enough to be called stand-alone single crystals (Figure **2**). Rather, they were textured columnar growth of diamond crystals with slight misorientation (2-6° tilt angles) with the substrate lattice planes (Figure **2I**). This tilt angle between the substrate and the epitaxial film was due to substrate surface roughness, defects, dislocations, ion bombardment during bias enhanced nucleation (BEN) etc.

The homoepitaxial substrates [17], i.e. high pressure high temperature (HPHT) or the natural diamonds, had many defects present inside and on the nucleation surface, which limited the perfect epitaxial growth of diamond. On the other hand, heteroepitaxy was predominantly governed by the lattice mismatch, resulting inevitable misorientation of the grown diamond crystals with the base substrate. Scratching of the substrate before deposition might cause surface damage which was detrimental to epitaxy. So, bias enhanced nucleation technique was adopted for enhancing the nucleation density before growth to achieve 10^{11}cm^{-2} nucleation density. Among different substrate material available, iridium (Ir) had the minimal lattice mismatch, so they could produce good amount of diamond epitaxial growth. Recently Ir has become the material of choice for large area (4 inch) growth of diamond single crystals other than trying tiling (Figure **2II**), lift-off etc. homoepitaxial techniques. Earlier the term single crystal synthetic diamond (SCD) was limited to high pressure high temperature (HPHT) diamonds. But with the advent of efficient CVD growth recipes and reactors (Table **1**, Figure **3**); SCDs are also sourced from CVD reactors. Table **1** summarises the state-of-the-art CVD techniques for growing single crystal diamonds. There are many research groups around the world who are developing new techniques and methods for continuous advancement in this field. Michigan State University, Carnegie Institute of Washington, USA, LIMPH, France, Bristol University, Element Six, UK, Beijing University of Science and
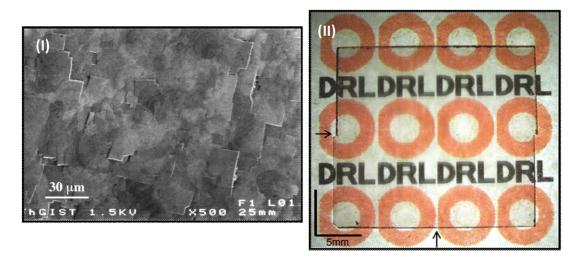

Figure 2: (**I**) heteroepitaxial diamond films on silicon with 30µm lateral size, developed during 1990s [15], (**II**) recently developed 20×40 mm^2 SCD tiled clones [56].

Technology, Wuhan Institute of Technology, China, AIST, Japan, IAP-RAS, Russia, Innovative plasma, Germany etc. are the names of the leading organisations.

2. MATERIALS & METHODS: CVD GROWTH OF SINGLE CRYSTAL DIAMOND (SCD)

2.1. CVD Reactors and SCD Growth Rates

There are several diamond groups all over the world, who are designing and manufacturing reactors for efficient and fast production of diamond by CVD techniques. They are exploring new recipes and efficient plasma formation for rapid SCD growth. During the initial SCD growth years, it was believed that introduction of nitrogen into the CVD recipe would enhance the growth rate of diamond over HPHT single crystal seeds but the results were not very encouraging as the grown SCDs were yellow in color and were not useful for electronic applications. So the research effort was put into making colorless purer SCD by high pressure high power density microwave plasma CVD. It was found that using very high methane percentages at high pressure would rapidly grow SCD and high microwave power density ensured dissociation of precursor radicals effectively. Table **1** summarises such efforts and their findings in making SCDs in recent years. Figure **3** shows snapshots of different reactors capable of producing SCDs.

2.2. Growth Theory of SCDs

Homoepitaxial growth of diamond under microwave assisted plasma CVD with addition of nitrogen in the methane-hydrogen precursor gas mixture at ppm level (Figure **4III**), could result (100) oriented single crystal diamonds. But addition of nitrogen introduces defect in the diamond lattice which produces coloration of the SCDs. To produce, white diamond, it is required to prevent nitrogen from going inside the diamond lattice, by using leak proof reactors with very pure precursor gases. High power high density plasma could produce SCD at high growth rate even at high methane percentages (Figure **4I**). But the exact mechanism of CVD diamond growth is still not clear because of lack of probing technique which could reliably give in-situ information of diamond growth environment. Researchers at the University of Bristol, LIMHP, France, Naval Research Laboratory, USA etc. have done pioneering work in understanding the diamond growth mechanism. Microwave generated plasma dissociates the precursor gas molecules into hydrogen and methyl radicals, which diffuse and react on the heated substrate to deposit diamond. CH_x and C_2Hy are the main precursor radicals for diamond growth. Nascent hydrogen helps in formation of diamond phase over other forms of carbon by preferential etching [114] of non-diamond deposits. Modelling and numerical simulations have been carried out to understand the microwave CVD growth of SCDs [115-117] as shown in Figure **5**. Optical emission spectroscopy and mass spectroscopy techniques [118] are used to probe the plasma. Hydrogen radicals are most prevalent under the typical

growth environment and it helps in formation of active site for adsorption of carbon radicals. Under high methane concentrations for growing SCD, it is the high density of microwave power that maximises hydrogen dissociation and promotes rapid growth of diamond (Figure **4I**). Other than microwave plasma assisted process, DC plasma torch also have been tried for higher growth rates (Figure **4IV**) but purity of the film can not be guaranteed. It has been observed that addition of N_2O can greatly enhance the SCD growth rates (Figure **4V**) but again the contamination issue prevents usage of any other recipe for high quality SCD growth. It has been observed that due to the presence of nitrogen vacancy centres, colorless crystals are not formed which further limits its electronic applications. Homoepitaxial growth can be explained by Figure **6**, where it is evident that there exist three growth modes: lateral growth, 2D island growth and 3D growth, when the methane concentration is increased from 0.005% to 0.25% gradually. Growth of atomically flat surfaces is very important for realising electronic grade diamond materials. SCD crystals are often found with growth hillocks (Figure **7I**), step/terrace and also when they are etched with oxidants, dislocations can be traced back for etch pits. Such defective surfaces are detrimental for end engineering applications. So it is essential to remove such growth defects in SCDs either by pre-treatment of the substrate or by using proper growth parameters. The seed substrate must be smooth enough for producing defect free SCD surface [119]. However there are polishing techniques which can produce atomically flat silicon substrates but producing atomically flat diamond [120] seed substrate needs further research. Growth hillocks (Figure **7I**) are formed due to preferential spiral growth at the site of screw dislocation in seed substrate, which are invariably present (10^4–10^5 cm^{-2}). SCD grown by CVD unavoidably has bundles of edge dislocations lying parallel to the [001] growth axis. Strain induced birefringence pattern shows four bright petals with dark arms along <110> for polarizer parallel to <110> directions. But it changes to eight petals of weaker intensity with dark arms along <110> and <100> directions for polarizer parallel to <100> [121]. High-quality crystal with a flat surface (Figure **5II**) and a low defect density is necessary for the stability of power-devices with low leakage current. Two dimensional local stress distribution in an epitaxial diamond layer had been studied and was found to be between −93 to +40 MPa around a dislocation with the assumption that the Raman peak shift [122, 123] image of the zone-center optical phonon was shifted at strained areas by 3 cm^{-1}/GPa. Selective masking by Pt nanoparticles of the existing defects on the substrate surface is to prevent threading dislocations propagating into CVD grown diamond layers. The steps that are followed: a) etch pit (EP) formation at the outcropped defect sites on the HPHT substrate surface by H_2/O_2 plasma treatment at 830 °C for 90 min with working pressure of 200 mbar and a microwave power of 3 kW, b) 10-50nm Pt interlayer deposition by MOCVD, c) Platinum film dewetting (H_2 plasma and 800 °C, a microwave power of 3 kW and a pressure around 200 mbar in CVD reactor) to match Pt nanoparticle

Table 1:   CVD Deposition Groups and their Techniques for Growing SCDs [18-38]

Group of Researchers	Type of Reactor	Type of Substrate	Precursor Recipe	Pressure	Power (kW)	Power density (W/cm^3)	Substrate Temperature ($^{\circ}$C)	Growth rate (µm/hr)	Relevant Figures
Michigan State University, USA [39-45]	Cylindrical resonant cavity, hybrid modes – reactors A, B, C types	HPHT Type Ib SCD seeds with H_2 plasma cleaning	5-9 CH_4/H_2% (0-200ppm N_2)	180-300 (Torr)	2	100-1000	950-1300	20-75	Figures 3(IX), 3(XI), 4(I), 7(IV)
AIST, Japan [46-56]	AsTEX/Seki, sometime with open or close type Mo substrate holders	HPHT Type Ib SCD seeds	12 CH_4/H_2% (0.12% N_2/H_2)	160-180 (Torr)	2-3	100-150	1130-1150	30-50	Figures 2(II), 3(VII), 4(II), 10
LIMHP, France [57-68]	LIMPH	HPHT Type Ib SCD seeds	2-7 CH_4/H_2% (0.02% N_2/H_2)	100-200 (Torr)	2-4	60-130	800-1000	5-55	Figure 3(I), 4(III), 5(I, II)
Carnegie Institute of Washington, USA [69]	AsTEX/Seki	HPHT Type Ib SCD seeds	8-22 CH_4/H_2%	100-200 (Torr)	3-5	50-100	1100-1300	50-100	Fig. 8(VIII)
IAP-RAS, Russia [70-74]	MSU- Type A	HPHT Type Ib SCD seeds	1-12 CH_4/H_2%	50-250 (Torr)	2.7	80-200	900	1-20	Figure 3(XI)
Beijing University of Science and Technology, China [75-81]	2.45GHz, Dome shaped, TM_{021}, Cylindrical cavity, Ellipsoidal cavity with circumferential antenna	Si (no SCD growth)	6	15kPa	8.5	-	950	3.5	Figure 3(II), 3(IV), 3(V), 3(X), 3(XII)
Wuhan Institute of Technology, China [82]	TM^{021}, 2.45GHz, multi mode	Si (no SCD growth)	0.6–5.0 CH_4/H_2%	6 kPa	4.5	-	900	8.5	Figure 3(II)
Bristol University, UK [83-88]	2.45 GHz reactor of Element Six, quantum cascade laser for measuring C_2H_2 and CH_4 column densities	Theoretical numerical modelling of CVD diamond growth	4.5 CH_4/H_2% (7% Ar) 565sccm	150 Torr	1.5	20-40	700	Cavity Ring Down Spectroscopy (CDRS) for C_2, CH, H species	-
Element Six, UK [89-91]	2.45 GHz	{001} type IIa HPHT	5.5 CH_4/H_2% with 10% argon (700sccm)	>15kPa	-	-	830		-
DC arc jet [92-94]	DC arc jet for 3 - 12 hours	IIa natural SCD or HPHT Ib with acid and plasma etching for defect removal	0.5-2.5 CH_4/H_2% (no N_2) (2-6 slm of Ar and 2-8 slm H_2 each)	8-8.5kPa	20-30	-	900-1030	15-60	Figure 3(VIII), 4(IV)
Stress removal by depositing metal island on substrates [95-97]	e-beam evaporation of 20 nm thick Ni, Au, Pt islands for 0.17-10 hrs	(111) HPHT seeds, wet acid cleaning, ultra so-nication, plasma etch	0.5 CH_4/H_2%	80 (Torr)	0.8-1.2	-	900-950	2.5-6.25	Figure 7(III)
Iridium heteroepitaxy [98-105]	2.45 GHz; BEN: 30-60min, 50-300V negative bias, 850°C, 20-40mbar, 700-2100W microwave power with 1-10% CH_4 in H_2; 30hr of diamond CVD	Ir/SrTiO3 or Ir/YSZ/Si (100) 1 inch size	1 or 7 CH_4/H_2% sometimes with 40 ppm N_2	30 – 50 mbar	1.1-2	-	800	0.43 or 1	Figure 3(VI)

Awadesh Kumar Mallik

(Table 1). Continued.

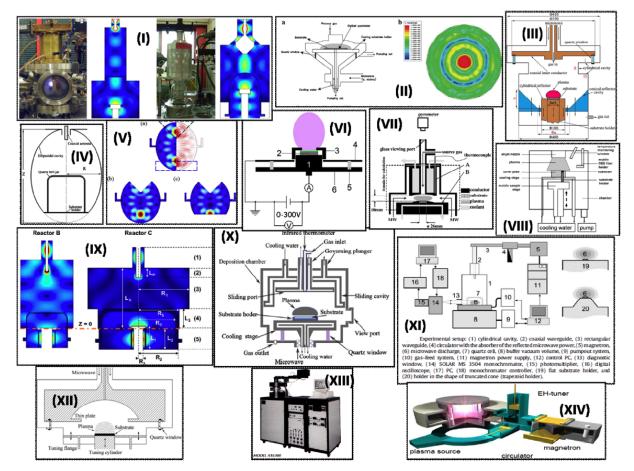| Group of Researchers	Type of Reactor	Type of Substrate	Precursor Recipe	Pressure	Power (kW)	Power density (W/cm^3)	Substrate Temperature ($^{\circ}$C)	Growth rate (µm/hr)	Relevant Figures
High growth rates with addition of N_2O and CO_2 gases [106, 107]	ASTeX 5250, 2 h.	3×3×1mm^3 HTHP synthesized type Ib (100)	12 CH_4/H_2% (0-10 sccm of N_2O gas); $CH_4/H_2/N_2$ (60/500/1.8 sccm), CO_2 0-30 sccm	300; 120 (Torr)	2	-	1100; 1000	135; 45-70	Figure 4(V)
HFCVD [108-111]	sp3 Diamond Technology Inc., W impurity levels 1.8×10^{18} and 1.2×10^{19} cm^{-3} at the grown surface and interface region	HPHT-grown type Ib (001) and MPCVD-grown (001) substrates (cleaned in boiling acid mixture), ion C^+ bombardment for lift-off technique	3 CH_4/H_2%	30 (Torr)			W filament, 2100 $^{\circ}$C, 10–15 mm substrate filament distance, 38hrs run	Not reported	65/38= 1.71	Figure 7(I), 7(II)

Figure 3: PECVD reactors for SCD growth, (**I**) electric field distribution inside metallic-chamber with belljar, co-developed between LSPM and Plassys company, showed opened on the picture [63], (**II**) Multimoded reactor, the two primary modes of TM$_{01}$ and TM$_{02}$ overlap around the substrate, weak area of TM$_{01}$ is the strong area of TM$_{02}$ making large plasma ball [31, 82], (**III**) with conical-reflector [32], (**IV**) Ellipsoidal cavity type reactor at Beijing, China [80], also AIXTRON type has similar configurations, (**V**) to transform circumferentially fed ellipsoidal cavity into an MPCVD reactor. From(a) to (c), an upper and a lower part of the cavity are removed, with the resonant pattern of the remaining cavities unchanged, at Beijing, China [79], (**VI**) with bias enhanced nucleation (BEN) for Ir heteroepitaxy, 1) Sample post, 2) sample, 3) Mo cap, 4) grounded Mo plate, 5) ceramic spacer, and 6) bias plate [98], (**VII**) flat plasma at AIST [49], (**VIII**) DC arc jet plasma enhanced chemical vapor deposition [92], (**IX**) hybrid reactors (B type-TM$_{013}$/TM$_{001}$; C type-TM$_0$/TM$_{001}$) at MSU [39], (**X**) newly built TM$_{021}$ mode cavity type MPCVD reactor at Beijing, China [78], (**XI**) MSU Reactor type A [71], (**XII**) Dome-shaped cavity type reactor at Beijing, China [77], (**XIII**) ASTeX/Seki type reactor [112], (**XIV**) iplas cylindrical reactor with annular slot [113].
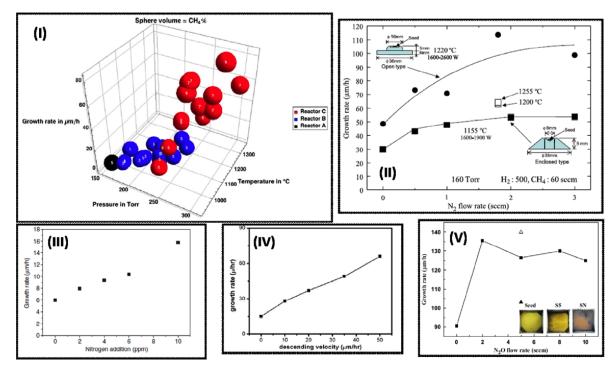
Figure 4: Growth rates for SCDs in (**I**) MSU reactors without nitrogen addition [44], (**II**) AIST reactor as measured by weight as a function of the nitrogen flow rates [50], (**III**) LIMHP reactor as a function of nitrogen addition in the gas phase [68], (**IV**) DC arc jet plasma enhanced chemical vapor deposition [92], (**V**) with N_2O addition [106].
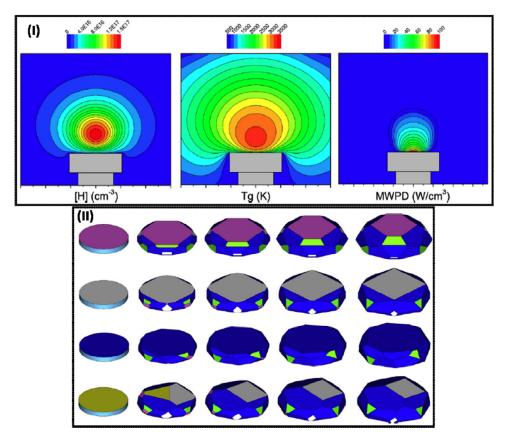

Figure 5: SCD growth simulation and modelling at LIMHP reactor, (**I**) spatial distribution of atomic hydrogen density ([H]), gas temperature (Tg) and microwave power deposition (MWPD) deduced from 2D self-consistent modelling of a pure hydrogen plasma [59] (**II**) Modelling of epitaxial growth of diamond films for increasingly longer deposition times, from left to right, for cylindrical substrates with different orientations (from top to bottom: [1 1 0], [1 0 0], [1 1 3], and [1 0 0] misoriented by 10° along the [1 1 0] direction) [58].
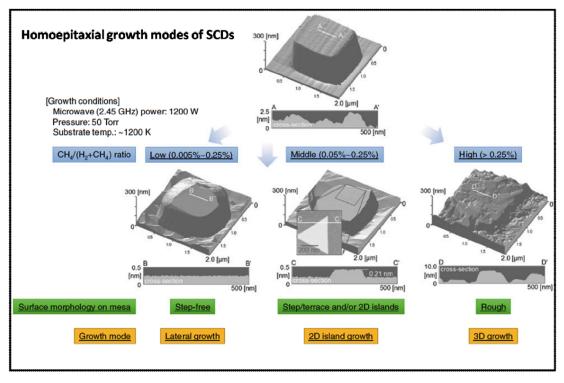
Figure 6: AFM images of the growth modes for producing atomically flat, step/terrace, rough SCD surfaces [17].
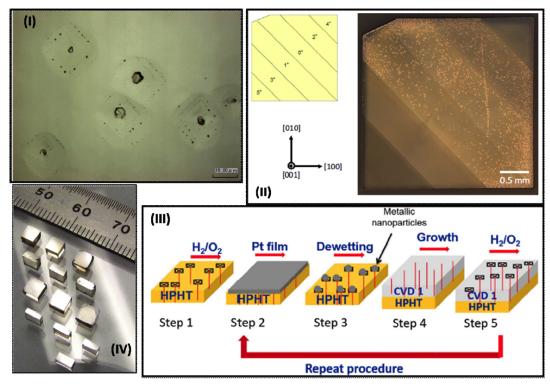

Figure 7: SCD growth defects and methods for arresting them, (I) Laser microscopy image of the nanocrystals and pyramidal hillocks [108], (II) schematic image of the substrate possessing different vicinal (001) off-axis angles from 0° to 5°; >2° misorientation angle produces hillock free SCD surface [108], (III) selectively mask substrate defects with metallic nanoparticles in an attempt to decrease dislocation densities [97], (IV) examples of SCD plates grown by MWCVD [39].

deposition only on EP, d) 80µm SCD growth again followed by, e) H_2/O_2 plasma treatment for revealing new etch pits. This cycle (steps a-e, Figure **7III**) repeats successively for

better control of dislocations (less number of EPs) on the final top surface [124]. Another method of reducing defect or dislocation density on the top surface of the growing SCDs is

to use pyramidal shape substrates. The original pyramidal-shape tends to disappear after a certain thickness is grown. The 20° inclined faces of the pyramid deviated dislocations towards the edges of the crystal, hence limiting their occurrence at the surface [125]. However, complete suppression of growth hillocks are possible by using highly misoriented (>2°) substrates (Figure **7II**). Atomically flat step-free SCD surface can be formed with mesa fabrication followed by lateral growth mode with very low methane concentration [17].

2.3. Doping of SCDs

Diamond is electrically insulating but with appropriate doping it can become semiconducting or even superconducting. P-type doping with boron [126, 127] is not difficult but it has been found that doping diamond with nitrogen for semiconducting purposes is not possible, as the size of N_2 atom is bigger and it is associated with the diamond lattice as different color centres. It is now phosphorus which is being used for n-type conductivity in diamond electronics. H_2-diluted (1%) CH_4 gas containing $P(CH_3)_3$ with P/C ratio of 0.99% at substrate temperatures 960-1210°C was used for homoepitaxial diamond growth of phosphorus (P)-doped films on vicinal (001) substrates with misorientation angle of 5° using high-power-density microwave-plasma chemical-vapor-deposition (MWPCVD), for making deep ultra violet light emitting diode [128, 129]. CL peaks were observed in the UV and visible regions, indicating further improvement of crystalline quality of the P-doped diamond film was required for observing monochromatic deep UV light emissions, with reported rectification ratio of about 10^3 at ±20 V. On the other hand, p-type doping with boron is well established for CVD grown diamonds. Ramamurti *et al*. deposited 1–2 mm thick boron-doped diamond with an electrical resistivity of 13 Ω-cm at a growth rate of 8–11.5 µm/h, using 1 ppm diborane in the feed gas as the boron source, in 30-45 W/cm^3 power density plasma CVD. Boron doping was also carried out by boron ion implantation at the acceleration energy of 80 keV with two different doses of 5×10^{14} and 3×10^{15} cm^{-2} on 125-350µm thick SCDs at microwave power density of 200 W/cm^3 inside a 2.45 GHz MPACVD reactor using natural diamond seeds (type IIa). Rapid annealing at nitrogen atmosphere, at 1380°C, was used to recover the damaged layer and to activate dopants in the CVD diamond. B-implanted diamond

layer showed, 1150 cm^2/V.s mobility at 300 K and a surface resistivity of 13.3 kΩ/sq, with surface N_s concentration of 4×10^{11}cm^{-2} [130]. High microwave power density (100W/cm^3) was found not to promote boron doping even at high concentration in gas phase (leading to plasma instability) while, low power density (<50W/cm^3) could increase doping efficiency but at the expense of twinnings and other growth defects appearing on the surface. It has been shown that at moderate plasma power density, thick heavily B-doped diamond crystals >10×20 cm^{-3} with good morphologies can be produced [131].

3. DISCUSSION OF PROPERTIES AND APPLICATIONS OF SCDs

Single crystal natural diamonds had been in demand for its aesthetic value since ages and were being mined from the earth's crust. There are ethical issues like "blood diamond" being involved in mining of diamond with cheap labour. Moreover HPHT and earth mining are more expensive and technologically challenging than CVD grown diamond. But there is a great demand-supply gap of SCDs due to their unique properties. The most profitable one among them is for the gem industry. But other than jewellery, there are many technological blockades due to non availability of suitable material. Diamond has the highest thermal conductivity, young's modulus, and acoustic velocity, wear resistance, chemical and biological inertness, radiation hardness to name a few. Many of these properties can be utilised to achieve next technological revolution (Figure **8**). For example, new era of high power electronics can be realised using SCD based switches (Figure **8III**), with very high breakdown voltage, which is to be used in power transmission grids. There are many other properties (Table **2**) like the presence of negatively charged nitrogen vacancy centre for realising quantum computation, high thermal conductivity for efficient heat dissipation in high power laser windows, which are seeing exponential rise in terms of number of publications in recent years.

3.1. SCD Detectors (Figure 9)

Diamond has several advantages over existing Si semiconductor. It has a wide band gap of 5.45eV in compare to 1.12eV for Si, which makes them to be used for high

Table 2:   SCD Property and Applications

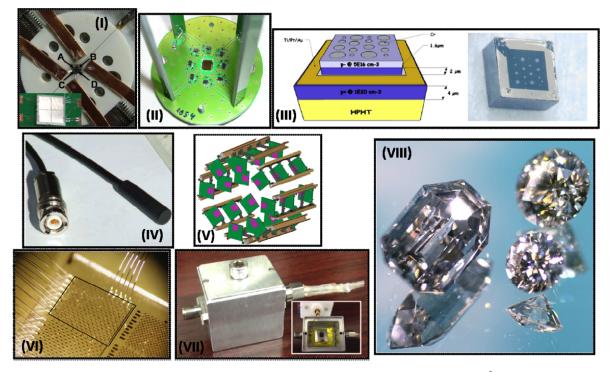| Property	Values	Application
Radiation hardness	43eV	Particle detector
High breakdown voltage	>10MV/cm	High power switches
Single NV⁻ centres	1.96eV	Quantum information
Mechanical hardness	130GPa	High pressure anvils
Aesthetics	Color, clarity	Jewellery
High thermal conductivity	22W/cm.K	High power laser window
High electron and hole mobility	4000 cm^2/V.s	High Power electronics

Awadesh Kumar Mallik

Figure 8: SCD applications: (**I**) X-ray detector [143], (**II**) PC board (=50mm) with the diamond (4.7× 4.7mm^2) in the centre surrounded by 8 amplifiers, for detecting time of flight of MIP [146], (**III**) Schottky barrier diode for high power electronics [179], (**IV**) SCD dosimeter within casing, [161], (**V**) Pixel Luminosity Telescope (PLT) with SCD sensors for LHC upgrade [138], (**VI**) SCD 3D particle tracker [141], (**VII**) detectors used in CMS and ATLAS detection locations of LHC [slide presentation, Jared M Smith, 2014], (**VIII**) near colorless and colorless single-crystal CVD diamond specimens, clockwise from the top: 1) Light brown, brilliant cut and polished single crystal containing nitrogen (~0.5 carat); 2) Near colorless, 0.2 carat brilliant cut and polished single crystal produced from a ~1 carat block; 3) Colorless 1.4 carat bullet shape single crystal produced from a ~2.2 carat block [69].
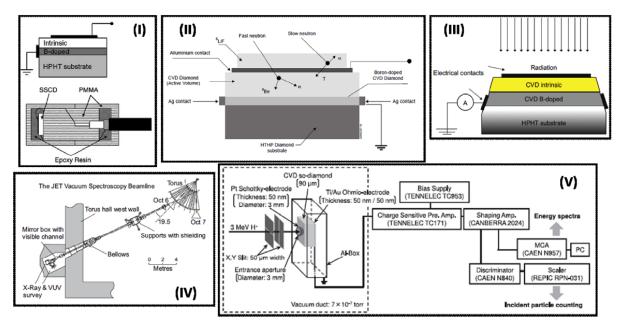

Figure 9: (**I**) Single crystal CVD diamond dosimeter [155], (**II**) diamond mosaic crystals for neutron instrumentation [152], (**III, IV**) SCD detectors for VUV and soft X-rays measurements on JET thermonuclear fusion plasma [148], (**V**) schematic of diamond detector and block diagram of the electronic circuit used in 3 MeV-proton measurements [144].

temperature semiconductor with less leakage currents. The thermal conductivity of diamond is 22 W/cm.K, which does not necessitate having extra cooling arrangement as in Si (1.5W/cm.K) devices. Diamond has very high electron and hole mobilities of 2200 (for Si 1450) and 1600 (for Si 500) cm^2/V-sec respectively, giving rise to fast signals. But it has

high electron-hole pair creation energy of 13.6eV and low mean electron-hole pair by MIP of 36 per 1μm – giving rise to smaller signals. Although single crystal diamond gives 100% charge collection efficiency (CCE) but polycrystalline diamond has limited charge collection distance (CCD) due to recombination of the generated electron hole pairs before reaching the electrodes. Diamond has moderate dielectric constant of 5.7 (Si 11.9) which gives less capacitance and noise. The most important property of them all is the radiation hardness of diamond is very high (43eV atomic displacement energy whereas Si has 21eV). The diamond detectors (large area pads: calorimetry; microstrips; pixel detectors (Figure **8V**)) when used under the radioactive environment of particle physics experiments, it has shown to sustain high fluence of pions, neutrons, electrons, protons, gamma rays, alpha particles etc under high beam energies [132-138]. SiC although being radiation hard and can be used at high temperatures but due to its interaction with neutrons, it can not be used as detector in the event of nuclear reactor accidents. Diamond retains semiconductor properties even if the reactor core is melted. Tsubota *et al*. have shown that SCD detectors from Diamond Detector Ltd. can be used at 523K [139]. CMS and ATLAS detection locations in Large Hadron Collider (LHC) have diamond based detectors (Figure **8VII**) [140]. The aim of the experiments was to detect new and rare high energy particles in LHC accelerator with maximum energy of 7TeV. It has been recently reported that the next upgrade of particle detectors in LHC may not be made of diamond as it has shown to degrade charge collection efficiency after exposure to proton irradiation from Polonium-210 alpha source. The author has also hinted that the future detectors may be based on 3-D diamond structures (Figure **8VI**) [141, 142]. Prototype single-crystal quadrant detectors for the X28C beamline at the National Synchrotron Light Source (NSLS) have provided the ability to simultaneously resolve the X-ray beam position and obtain a quantitative measurement of the flux (Figure **8I**) [143]. Single crystal diamond (Figure **9V**) was tested to determine 3 MeV protons generated by a pelletron accelerator for possible fusion reactor plasma diagnostic application [144, 145]. 4.7×4.7 mm^2 SCD were irradiated with proton beams with kinetic energies from 1.2 to 3.5 GeV and with rates upto $3×10^6$/s.mm^2 for HADES spectrometer (Figure **8II**) [146]. Single crystal CVD diamond based photo-detectors, for extreme UV detection and for soft X-ray radiation, have been successfully installed at JET for possible future applications in ITER (Figure **9III**, **9IV**). The detectors installed in the Vertical Port (Oct-1), Oct-1 Limb 1/2 and in the main horizontal port (Oct-6) of JET are 200μm, 104μm and 75μm thick respectively and are embedded in paraffin or covered by a thermally evaporated 3 μm thick ^{6}LiF film, surrounded by 2.5-cm-thick polyethylene. They have a detection efficiency of about 2.9×E-05 counts/n×cm^2 for the 14MeV neutrons [147, 148]. Three dimensional graphite pillars [149] buried within single crystal diamond detectors by a femtosecond IR laser, have been demonstrated to be efficient charge collector when impinged with ^{90}Sr, Y β-particles [150]. Femtosecond laser

ablation technique has also been used to produce statically bent diamond single crystals for possible optimal solutions for crystal-based collimation and/or extraction [151]. Neutron diffraction experiments when performed on single crystal diamond samples, 34% peak reflectivity has been obtained for a 1 mm thick crystal at 1˚A wavelength (Figure **9II**) [152]. One large size single crystal diamond, prepared by "lift-off" techniques, when used as sandwich type detector, showed 98% hole charge collection efficiency whereas for electrons, CCE was 89% when irradiated with 5.486 MeV α-particles [153, 154].

Natural diamond dosimeter is very costly, rare and dose rate dependant, whereas CVD grown polycrystalline diamond or HPHT synthetic diamonds are defective to be used as dosimeter for radiotherapy (Figure **9I**). Intensity Modulated Radio Therapy (IMRT) is created to form highly conformal dose distributions and to reduce unwanted irradiation of surrounding healthy tissues. Single crystal diamond (SCD) has all the properties of ideal dosimeter, like human tissue equivalence, radiation hardness, stability, linearity, high sensitivity and independence from energy and dose rate, other than having fast response time and high spatial resolution. Single crystal diamonds in p-type/intrinsic/metal (PIM) structure has been found to be effective in photovoltaic regime developed at University of Rome "Tor Vergata". 6 and 10 MV Bremsstrahlung X-ray beams and electron beams, from 6 MeV and upto 18 MeV, obtained by a CLINAC DHX Varian accelerator, were used for their characterisations. Water phantom and commercial ionization chambers were used for calibration and comparison with commercial dosimeters [155-158]. Other than x-ray and electron beams [159] such Schottky diode detectors have also been tested for small field [160] photon beams in clinical radiation therapy (Figure **8IV**) [161]. Moreover the same PIM structure had been irradiated with 20nm to 100nm UV and EUV radiation with very good photoconductivity, without undesirable memory effect, good response time and high signal to noise ratios [162].

Ultra-high power free electron lasers (FELs), Energy-recovery linac (ERL) light sources, electron cooling of LHC may need SCD amplifier for generating high-current, high-brightness electron Beams [163].

Thermonuclear fusion reactors need 1 MW continuous wave power source at 170 GHz frequency for plasma heating. Such high energy transmission necessitates large diameter diamond window for efficient thermal management and also low loss transmission [164]. So far large diameter polycrystalline diamond windows [165-167] have been used but they have grain boundaries which affect the transmission loss. So the best window material would have been large area single crystal diamond but synthesis of inch size SCD is still a technological challenge. Attempts have been made, to characterise by Fabry-Parot method, the rectangular tiled clones of SCDs, made by lift-off technique (Figure **10**), for evaluating their possible future use in Gyrotron window
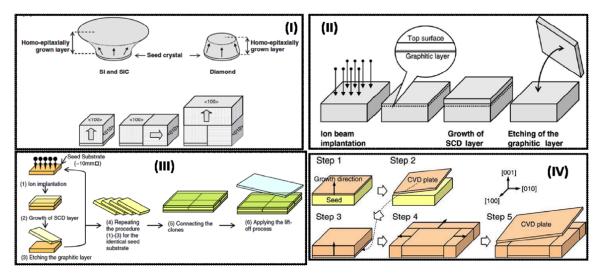
Figure 10: Scaling up of lateral dimension for large area SCD growth: (**I**) enlargement of the area during the crystal growth as in the cases of Si and SiC, whereas, shrinking of the area during the crystal growth in the case of single-crystal diamond (SCD) due to introduction of nitrogen in the feedstock gas; 3D-growth of SCD to grow in dimension [46], (**II**) Lift-off process with ion implantation: high energy ion beam is injected onto the top surface of the substrate, and graphitic layer is generated beneath the top surface, after this process SCD layer is grown onto the identical top surface, by etching the graphitic layer selectively, SCD layer is made freestanding wafer, [46], (**III**) procedure to produce clones and tiled clones [56], (**IV**) size increase of crystal by repeated lateral growth [54].

application [168]. It was found to show tanδ 10^{-5} for $20 \times 20 mm^2$ tiled clones but for $20 \times 40 mm^2$ tiled clones the tanδ was equal to 10^{-4} at the central part of the SCDs with 5.7 dielectric constant.

3.2. High Power Electronics

Diamond has a very high breakdown voltage which makes them effective for Schottky barrier diodes (SBD) or pseudo Schottky diodes (pSBD). FACTS (Flexible AC Transmission Systems) contains tens of silicon Insulated Gate Bipolar Transistors (IGBTs) in series with giant cooling arrangements. Low operating temperature of 150°C and very low thermal conductivity of 1.5 W/cm-K makes silicon inappropriate for making any improvement in the present electrical delivery systems and power converters, in order to provide a more efficient conversion of their output power into a form that is suitable for grid connection. Materials having superior properties over silicon are obvious alternatives for the next advancement in energy technologies. Wide band gap semiconductors like SiC, GaN having higher thermal conductivity and breakdown voltages are now in the process of commercialisation for such applications. But diamond's highest thermal conductivity, breakdown voltage combined with wide bandgap, high electron-hole mobilities (4500 and 3800 cm^2/V.s for electrons and holes, respectively) at room temperature, low dielectric constant, and chemical inertness make it the ideal material of choice for high power high temperature electronics. Diamond shows extremely high Baliga's figure of merit (BFOM) or Huang's FOM compared with SiC or GaN for high-power and low-loss performance or high power switching. Specific-on-resistence of SiC is better or comparable with diamond at room temperature due to higher carrier concentrations, but at elevated temperature,

when electron are scattered by phonons [169], the diamond performs better than SiC as its carrier concentration increases. 90% reduction of power loss has been estimated by using diamond SBDs instead of SiC SBDs in high temperature applications. But boron doping with 0.36eV and phosphorus doping with 0.6eV activation energies make low carrier concentrations at room temperature. Boron can be easily doped from 10^{18} to 10^{21} cm^{-3} concentrations whereas doping phosphorus into diamond cubic crystal is major (size) problem. Many types of unipolar diodes (Figure **8III**) so far have been reported [170-185].

High values of microwave power density is good for high quality rapid growth of SCDs, but it reaches a boron doping saturation value of 10^{19} cm^{-3}, which could further be increased with increase of B/C ratio (>5000ppm) in precursor gas, but that leads to soot formation and unstable plasma. It has been found that 60 W/cm^{-3} plasma power density could give boron doping level of 3×10^{19} cm^{-3}. The vertical Schottky diode has I–V characteristics current density between 1000 and 2000 $A.cm^{-2}$, a rectifying ratio of 10^{10} and a breakdown electric field in excess of 1.3 $MV.cm^{-1}$, low leakage current and low on-resistance even at high temperature (250°C) conditions. 280 nm SiO_2 anti-reflection coating has also reportedly been coated by PECVD on both sides of 1.12 ct SCD with 98.7% transmission at 1.64μm for intracavity component in high power laser [186].

3.3. High Pressure Research

It has been found that boron doping also enhances the mechanical properties [187] of SCDs. Hemley *et al*. reported the growth of boron doped SCD by high density MPCVD at 5–20% CH_4/H_2, 0–0.2% N_2/CH_4, at 150–220 Torr and at temperatures ranging from 1100 to 1300◦C on commercial

HPHT synthetic Ib diamond plates (5 mm × 5 mm × 0.3 mm) with growth rates of 20–100 μm/hr. Hexagonal BN powders were kept in between Mo substrate holder and HPHT substrates for doping during CVD growth. Low pressure of 150-300 Torr and high temperature of 1600-2200°C was used for post-CVD annealing inside the same 6kW, 2.45 GHz CVD reactor. The fracture toughness of boron/nitrogen co-doped SC-CVD diamond was found to be between 22 and 34 MPa m$^{1/2}$ without compromising on its hardness of 88 GPa, whereas undoped SCDs after annealing gives very high hardness of 125 GPa and moderate K_{IC} of 12–16 MPa m$^{1/2}$. Boron has also found to reduce lattice defects giving PL spectra as good as type IIa diamond [188]. A single-crystal CVD diamond window for high-pressure SAXS cell was shown to perform well for high pressure research [189].

3.4. Jewellery

3.4.1. Color and Associated Defects

Diamond can be classified as type I and type II, based on the presence or absence of nitrogen (N) impurities inside the lattice. When the nitrogen atoms are aggregated inside, it is called type Ia, which further can be classified into type IaA (aggregated N pairs) and type IaB (aggregated 4N+V). Diamonds having isolated N atoms are called type Ib. But the absence of nitrogen or any other impurities make it very pure type IIa diamond. If there is presence of isolated single boron (B) atoms inside the diamond lattice, which makes it blue in color, it is called type IIb diamond [190]. Absence of any impurity makes the diamond colorless but it is the color which makes them attractive for jewellery purposes. Very common example of coloration is that the presence of nitrogen makes them yellow. There are as many as 500 types of defects, extended defects in natural/synthetic diamonds [191-196] but all of them are not important from gemological perspective. Yellow color (nitrogen atoms surrounding vacancy) in the visible spectrum is given by N3-415nm, N2-478nm, 480nm, H4-496nm and H3-503.2nm defect centres. Green color at 3H-503.5nm is given by interstitial carbon atom in the diamond lattice. Pink-to-red color in natural diamonds at 550nm is associated with plastic deformation of the diamond lattice. The popular defects centers NV^0 with absorption at 575nm and NV$^-$ centre with absorption peak at 637nm, also produce pink color. Another well studied defect centre, although outside visible spectrum is uncharged vacancy GR1 centre (irradiation with heavy ions) which gives green or blue colors with absorption at 741nm. H2 (986 nm) is often associated with H3 but gives strong green body color.

3.4.2. Industrial CVD of Gems

CVD growth rates were not high enough until recently for making gem size diamonds. But recent developments of high quality and high growth rate microwave plasma SCD technologies have raised immense interest among jewellery industry [197, 198]. Many lab-grown diamond companies are starting up, like US based Apollo Diamond (now known as SCIO diamond) [199], Gemesis Corp. [200], Washington

Diamonds, Microwave Enterprises, Singapore based IIa Technologies and many others all over the world. These are the new businesses based on CVD diamond technique, but before CVD, lab-grown diamond had been commercialised by HPHT techniques since early 1990s [201-205]. HPHT is very cumbersome process and it has inherent impurities from catalysts. Producing large size defect free diamond, in economical time frame is not possible by HPHT. Whereas, CVD diamond produces high quality colorless diamond, equivalent or even better than the best quality natural type IIa diamond [206] within reasonable duration. But before the advent of such high growth rate CVD processes in the past 10 years, there were coating attempts in utilising CVD diamond process for jewellery. But such efforts were to increase the aesthetics of the natural stones and with limited added value. Even the natural/HPHT diamonds were laboratory-irradiated with heavy ions for giving attractive colors to the stone [207]. Other than irradiation, CVD grown diamonds are also sometimes HPHT or low pressure low temperature (LPLT) treated for stress removal giving rise to different colors to the diamond stone. CVD grown 0.5 carat gems have been characterised by Gemological Institute of America (GIA) and it has been found to be as good as type IIa natural diamond. The color; shape; clarity; birefringence under crossed polarizer; green fluorescence in long, short and ultra-short UV radiation of DiamondView; blue phosphorescence at 550nm; FTIR absorption at 1332cm^{-1} and 1344cm^{-1} for N_s^+ and N_s^0 respectively; UV-Vis-NIR absorption band around 270nm with sharp peaks at 271nm and 268nm due to isolated nitrogen impurity; UV-Vis-NIR absorption doublet at 737nm due to [Si-V]$^-$; have been certified by GIA for lab-grown CVD diamond. Depending on the wavelength of laser excitation, Gemesis diamond has reportedly given PL zero phonon lines at, 737nm [Si-V]$^-$, 575nm [N-V]^0, 637nm [N-V]^0, 415 nm (N3), 451–459 nm (with HPHT post processing), 503.2 nm (H3), 946.0 [Si-V]^0, 882.7 and 884.4 nm (Ni related) wavelengths to prove the high quality of CVD grown diamond for jewellery industry.

3.5. Defect Centres

Photo luminescence (PL) emissions of nitrogen vacancy (NV) defect in diamond lattice (Figure **11I**) can exist in two charge-states, NV$^-$ and NV^0, with λ=638 nm and λ=575 nm zero phonon lines (ZPL), respectively. The inhomogeneous broadening of the ZPL NV$^-$ emission corresponds to a vibronic/phonon side band (PSB) transition with lifetime of 12 ns. Impurities and structural defects inside diamond lattice lead to variations in strain and electric fields, causing large broadening in PL spectra (Figure **11II**). Whereas, silicon vacancy (SiV) centres (Figure **11IV**) has ZPL at 738 nm and can be created by ion implantation or by in situ doping during CVD [208, 209].

3.5.1. Bulk NV Centre Synthesis

NV centre [210-213] is created in a diamond crystal containing nitrogen and vacancy defects with thermal
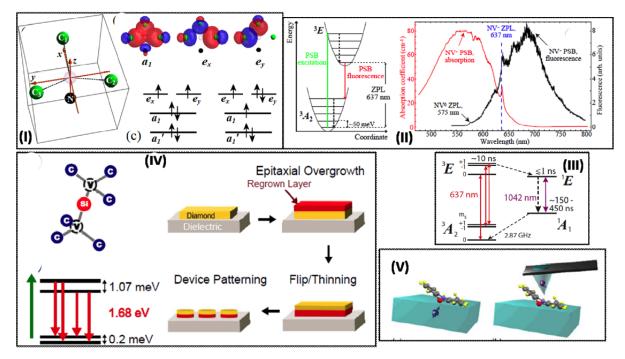
Figure 11: (**I**) Molecular orbital schematics of the NV center with nitrogen, vacancy, and three nearest neighbour carbon atoms with six electron spins at ground and excited states, (**II**) schematic illustrating excitation and fluorescence of the main optical transition while non-radiative decay is shown with dashed lines, with [NV⁻]~15 ppm, PSB–Phonon sideband, ZPL–zero-phonon line, (**III**) level diagram for the NV center showing spin-triplet ground and excited states, as well as the singlet system involved in intersystem crossing. Radiative transitions are indicated by solid arrows and non-radiative transitions by dashed arrows, lifetimes of the excited levels are also shown [236], (**IV**) SiV defect structure in diamond, energy level diagram, fabrication process of the resonance cavity [285], (**V**) magnetic field sensing from the nuclear spins of a molecule using a single NV⁻ center, either embedded or on a tip [215].

annealing at temperature ≥600 °C, when the vacancies start migrating to the nearest substitutional nitrogen atoms where their aggregation is energetically favourable. Defect concentration in SCDs can be controlled by thermal treatment (below the growth temperature) and by ultraviolet irradiation for influencing optical absorption profiles. Thermal treatment reduces various broad absorption features {absorption bands at 270 nm (for 1.7eV - N_S^0), 360 and 520 nm}. Above ~500 K, electron paramagnetic resonance (EPR) spectroscopy shows a decrease in the concentration of N_S^0 centres and a concomitant increase in the negatively charged nitrogen-vacancy-hydrogen complex (0.6–1.2eV for NVH⁻) concentration. But the ultra violet illumination recovers back the lost defects due to thermal annealing. Since the loss of N_S^0 concentration was greater than the increase in NVH⁻ concentration, it was suggested, that another unknown acceptor, existing at a similar energy as NVH, was present [214]. 1.8ms of spin dephasing time could be achieved by isotope engineering [215] of CVD diamond, which could detect magnetic field by single electron spin, where sensitivity was reaching 4 nT Hz$^{-1/2}$ with subnanometre spatial resolution [216-220]. It had also been found that NV centre could be created more effectively with low energy electron beam (2-30keV) irradiation, in scanning electron microscope, of the already N₂ implanted diamonds, and with a subsequent thermal annealing at 800°C for 15 min under 10⁻⁷ Torr vacuum [221, 222]. GR1 (uncharged vacancy) centers in diamond, formed by ion implantation of 2 MeV He ions over a wide range of fluencies, also give zero phonon line at 742nm [223].

Layered diamond structures with NV⁻ color centres were also fabricated either by doping/no-doping with N₂ (ppm) or it can be deposited by alternate pressure changes leading to temperature change in definite successive time intervals. In both the methods, authors [224] could successfully control the NV⁻ centre concentration of about >10¹² cm⁻³, but accurate depth control was not possible with only N₂ addition, due to long residence time of gases in the chamber, so it was concluded that alternate temperature variation alongwith constant N₂ doping is better option for efficient NV⁻ centre engineering.

3.5.2. Shallow NV⁻ Centre Synthesis

Nuclear spin, exterior to diamond lattice, has also been detected with shallow NV⁻ centres. NMR signal from single nuclear spins diminishes with the third power of distance, so single spin sensitivity can not be reached more than a few nanometers away from a sample. This limits the depth resolution and 3-D imaging of larger complex molecules. NV⁻ centres also get affected by surface defects due to their shallow implanted depth (>2nm). NV⁻ gets converted into NV⁰ [225] state due to surface charge [226] traps or band bending or optical illumination or by quantum tunnelling phenomenon, which can be controlled by terminating the surface with oxygen and fluorine or heavy nitrogen doping upto 5 nm

depth. Thin film magnetic impurities (dangling bonds) within 10 nm depth can affect spin relaxation time and causes noise in the signal.

20 keV $^{15}N^+$ ions implantation to sub-100-nm length scales was carried out (7 × 10^{15} cm^{-3}) into masked, high-purity CVD diamond substrates, with 30 nm size resist apertures patterned using a 100 kV electron beam lithography system. Successive annealing in Ar at 850 °C (induce vacancy diffusion to form NV^- centers) and then in O_2 at 420°C (reduce photochromism) did not promote diffusion of the implanted nitrogens for Toyli *et al*. [227].

Electronic grade single-crystal chemical vapour deposition diamonds (100) with a nitrogen background of <5 ppb from Element 6 were co-implanted with $^{14}N^+$, hydrogen, helium and carbon ions with low dose rate of 3×10^9 ion cm^{-2} s^{-1} and low beam energy of 7.7 keV to avoid irradiation damages by Schwartz *et al*. And then they were annealed at 780°C for 2 hrs in vacuum to enable vacancy movements for efficient NV^- centre formation [228].

3.5.3. Application of NV Centres – Diamond Photonics

One of the classical application of diamond NV centre is the diamond Raman lasers [229-234] for generating intense yellow light (573 nm) which corresponds to the peak absorption of oxyhaemoglobin for treatment of skin diseases. The NV^- centre [235] inside diamond lattice consists of substitutional nitrogen atom with a vacancy present at the adjacent lattice site. The luminescence from NV^- centre is very strong and stable. Moreover it can be optically detected with external magnetic field perturbations. This particular optically detected magnetic resonance (ODMR) property made this defect color centre of diamond a very important candidate for future quantum computers. EPR spectra of single NV^- centres has been detected by measuring the fluorescence intensity or ODMR [236-238] in response to microwave irradiation and, shift in EPR spectra can be caused by external perturbations of magnetic [239] and electric fields [240, 241], temperature [242], spatial orientation, strain [243], pressure, nuclear spin [244] and other physical parameters. Continuous wave (difference in frequency is measured at zero field), pulsed probe experiments (difference in frequency is measured with Ramsay Fringe) and spin relaxometry (in absence of microwave the relaxation time is measured under pump probe excitation) enable different sensing applications of NV^- centre in magnetometry. For example spin relaxometry can be utilised to measure paramagnetic ion concentrations in solutions. Shallow (<10nm) NV^- centres can be created on SCD plates by ion bombardment or thin film growth, for making sensor arrays for microfluidics or wide-field microscopy. Absolute orientation of nanodiamond spherical particles can be optically trapped and controlled by adjustment of light polarisation, using the vector dependence of the NV center on magnetic field. Cell membranes have different electric potential across them and that difference in

electric field potential can be detected by single nanodiamond embedded with NV centre. Nanoscale thermometry can measure temperatures in living cells by nanodiamond, with 10mK/√Hz sensitivity even at zero Kelvin and upto 200°C, using the temperature dependence of zero field splitting. NV^- centre can also react to change in strain or pressure which can further be used in high pressure anvil experiments or M/NEMS. Putting NV^- centre at the tip of a scanning probe over surfaces can produce images of the surface with separation as low as 2 nm (Figure **11V**). Either single nanodiamond [245] has been attached to AFM cantilever tip or single crystal diamond has been etched out to fabricate a tip. Another emerging application of diamond NV^- centre is nanoscale NMR [246, 247]. ^{13}C isotope naturally embedded (1.1%) in the diamond lattice has been placed in a higher magnetic field of hundreds of mT with detection of MHz Larmour precession of the nuclear spin.

Quantum computation [248] has now been realised at room temperature with long coherence time of diamond NV^- centres. At liquid helium temperatures NV^- can also act as optically addressable solid state spin qubits for quantum computation [249]. A fiber-based open Fabry-Perot microcavity incorporating a thick (>10μm) diamond membrane with NV^- emitters has been developed for cavity-quantum electro-dynamics application. Modified microcavity spectra has been observed in the presence of the membrane with Purcell enhancement [250] of approximately 20 for emitters within the diamond in such device [251]. Strong enhancement was achieved for the zero-phonon line of nitrogen–vacancy centers of a diamond micro-ring (4.5μm in diameter and 500 nm wide) coupled to a ridge waveguide (300 nm wide with spacing between the ring and the waveguide of about 100 nm). The zero-phonon line is efficiently coupled from the ring into the waveguide and then scattered out of plane by the grating outcouplers (Figure **12III**) [252].

3.5.3.a. Nanofabrication

Diamond photonics [253-261] is developing with advanced diamond nanomachining techniques. A top-down fabrication method [262] for realizing diamond nanowires (Figure **12I**) by inductively coupled plasma (ICP) reactive ion etching (RIE) with oxygen was used to fabricate the nanowires. Different masking materials like drop-casted Au, SiO_2 and Al_2O_3 nanoparticles as well as electron beam lithography defined spin-on glass and evaporated Au had been used. Al_2O_3 nanoparticles was the most etch resistant, while e-beam resist (spin-on glass) was suitable for fabricating ordered arrays of diamond nanowires with near vertical sidewalls in both polycrystalline and single crystal diamond. Single crystal diamond (types Ib and IIa) nanowires had the heights and diameters of 1-2.4 μm and 120-490nm respectively, with etch rates between 190-240nm/min.

ICP-RIE technique was again used on selectively Ti masked SCD substrates to produce different suspended nanobeam
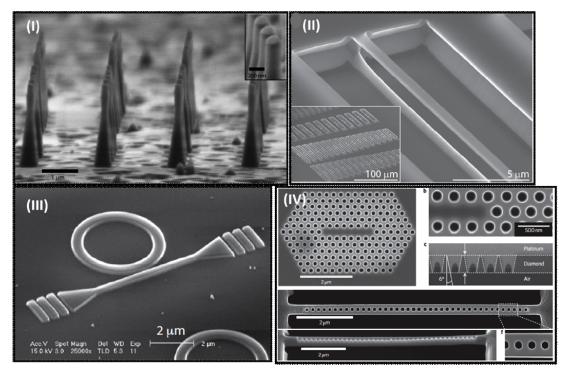
Figure 12: Single crystal diamond photonic structures: **(I)** *"nanowires"* obtained in a IIa CVD diamond [262], **(II)** *"nanobeam"* waveguide optomechanical system [276], **(III)** device consisting of a *"micro-ring"* resonator coupled to a ridge waveguide [252], **(IV)** SEM images of two-dimensional and one-dimensional fabricated PhC *"cavities"* [272].

structures like micros-disk, curved, spiral nanobeams, cantilevers, with isotropic angled-etching method using triangular or conical Farady cage, which may have potential application in optical resonators and nanomechanical assemblies. 700 W ICP power, 100 W RF power, 10mTorr pressure, 50 sccm O_2, and 2 sccm Cl_2 flow rates were used for 200nm/min top-down etching rate [263].

SCD dome resonator (an outer diameter below 10 μm and elevation of ~200 nm at the apex) was fabricated by ion implantation of HPHT Ib substrate with with carbon (energy 180 keV, dose 1×10^{16} cm^{-2}, forming 230-nm-deep sacrificial layer) followed by MPCVD of 100 nm thin SCD and electrolysis removal of the underlying stressed layer. Exceptional mass sensitivity or mechanical vibrational spectrum of the dome (thin shell clamped on periphery) exhibited a series of sharp resonances corresponding to different configurations of standing flexural waves that provided a diamond surface with the specificity toward analytes of interest, a superb choice for chem/bio sensing applications [264].

Single crystal diamond cantilevers and bridges, were fabricated by "lift-off" technique; followed by oxygen-argon RIE – with a photolithography procedure and; consecutively wet etching of the ion implanted sacrificial layer. Nanoindentation with atomic force microscopy revealed Young's modulus of 800 GPa whereas; the resonant frequency of vibration was 171 kHz. They could also be used as NEMS switches [265-267].

ICPRIE was also used to fabricate planar photonic crystal (PhC) cavities [268, 269] in nanocrystalline diamond with quality Q factor 2800. Nanometer thick silica layer was first deposited by plasma enhanced chemical vapor deposition (PECVD) on polished nanocrystalline diamond (NCD). Photonic crystal and the access waveguides were then patterned in electron-beam resist (spun on the surface) using electronic lithography. The pattern was successively transferred from the resist to silica (RIE) and then from the silica to the diamond (ICPRIE) with pure O_2 ions. HF acid was used to remove the rest of the SiO_2 mask. Vapor phase isotropic XeF_2 etching process was applied to etch 4μm of the silicon substrate to free the diamond membrane [270, 271].

Heteroepitaxial diamond films with a thickness of about 12 μm were grown by CVD on Ir/YSZ/Si buffer layer substrates. A free-standing membrane was then fabricated by removing the silicon substrate and buffer layers in small areas. Next, the membrane underwent reactive ion etching (RIE) in oxygen plasma to thin down from the nucleation side to a thickness of 300nm. Afterwards, the 1D or 2D structures (Figure **12IV**) were milled by a focused beam of Ga$^+$ ions (FIB) into the diamond film. The sample was annealed and cleaned after the milling process to recover a high-quality diamond layer [272].

Quidant *et al*. [273] fabricated V-groove plasmonic waveguides and coupled the NV centre emitters embedded inside with channel Plasmon polaritons. The emission from the nitrogen–vacancy centre is effectively guided for about 5

µm before being out-coupled into free-space propagating light, bringing plasmonic circuitary closer to reality.

It is difficult to build a photodetector directly out of diamond because of its wide bandgap, rigid lattice, and small lattice constant, for suitable detection of color center fluorescence. By combining diamond waveguides containing NV⁻s with a complimentary photodetector material, it is easy to detect NV⁻ centers emission with hybrid devices [274]. Diamond nanobeams (with less than 5 NV⁻ centre per beam) with triangular cross-section [275], 30-50µm long and 200-350nm wide, were fabricated by RIE oxygen plasma using Faraday cage and it was transferred, using a pair of 3-axis closed-loop piezoelectric nanomanipulators with sharp tungsten tips, to GaAs p-i-n structures for fabrication of hybrid photodetector. Barclay *et al*. demonstrated an inductively coupled plasma reactive ion etching (ICPRIE) process which did not require a Faraday cage, and instead utilized diamond undercut etching to fabricate nanobeams, from bulk single crystal diamond (Figure **12II**) [276].

3.5.3.b. Microfabrication

In-plane p-i-n structures (LED) were fabricated with (100) SCD crystal using lithographic masking and ion implantation of boron and phosphorus ions with energies of 70 keV & 95 keV and fluences of 2×10^{16} cm^{-2} & $\times 10^{16}$ cm^{-2} respectively. The electrical activation of the implanted boron and phosphorus was achieved by post implantation annealing in vacuum at a temperature of 1600°C for 10 h. The gap formed between the boron- and phosphorus-implanted domains (intrinsic, i-area) varied from 1 µm to 50 µm for different structures. These LED structures demonstrate electroluminescence of radiation-induced defects at the edges of p- and n-type areas and single-photon electroluminescence of individual NV⁻ defects in the i-gap [261].

Single crystal diamond pyramids with 4-5µm (100) base and triangular faces with 10-15 µm edge length were mass produced by DC arc-jet method and was demonstrated as AFM tip application [277]. Recently the same group reported mass production of diamond microneedles and its theoretical understanding [278].

Laser micromachining, by 355nm pulsed laser, of HPHT produced nano-polycrystalline diamond (NPD) and single crystalline diamond, revealed that two different mechanisms exist for NPD and SCD. Laser interaction with SCD forms microcracks and -cleavages, caused by the laser pulse itself and due to volume expansion involved in the diamond–graphite transition. In contrast, the laser interaction with NPD was grain-by-grain thermal ablation without any micro-cracks and lattice strains, and therefore the NPD cut surface was relatively straight and undamaged; whereas, the SCD had rough-edged cut surface [279].

Photoconductivity had been noticed with current flowing through the circuit when Ti/Au gates were patterned on HPHT

Ib SCD substrates with a potential across them, alongwith incidence of 532nm laser (2.3eV) [280].

Single-crystal diamond microdisk cavities (Figure **11IV**) were fabricated, from a single-crystal diamond membrane - generated by ion implantation and electrochemical liftoff followed by homo-epitaxial overgrowth, and afterwards ICPRIE thinning, to produce Si-V centre [281-283]. Si-V centres in the cavity has 1.8ns lifetime whereas the vacancy centres in the membranes (outside microcavity) has 1.48 ns lifetime [284].

4. CONCLUSIONS AND OUTLOOK

A comprehensive review of the current status of the single crystal diamond research has been carried out. The available reactors for growing SCDs and their respective capabilities have been presented concisely with tables and figures. The present understanding of the growth mechanisms of homoepitaxy have been outlined. The ongoing research activities in order to increase the SCD growth rates have also been described with graphs. Examples of real engineering applications of SCD, like particle detectors, high power electronics, high pressure anvils, gemology alongwith their working principles have been discussed. The most important of them all is the application of single NV⁻ centre for quantum computation which has briefly been touched upon. It is the first example of gate quantum computer that works at room temperature. The negatively charged nitrogen vacancy centre creates spin relaxation photoluminescence under green laser radiation. An external field can manipulate the spin orientation of the electron, recorded as resonance splitting, which can be controlled at a microwave resonant frequency of 2.87 GHz (Figure **11III**). Diamond chip can be placed on a microwave/radio frequency transmission line structure, and the chip's photoluminescence can be recorded as a function of the transmission line RF frequency. Manipulation of the single electron spin forms the basis of a quantum bit or "qubit". The NV⁻ qubit can function as a quantum logic gate in a circuit which can be programmed to perform calculations, forming a quantum turing machine. Classical computers are turing machines and can only change the bit logic gate between 0 and 1, one step at a time. Qubit exist in a superposition of 0 and 1 states. Hence the qubit can be used in an algorithm that uses all possible logic gates. There is exponential rise in diamond photonic research and vast numbers of articles have been published in leading scientific journals like Nature and Science in the past few years on NV⁻ centre. Photolumiscence property with application of different perturbation fields under room temperature conditions, with very long coherence time, has been exploited to make nanoMRI, strain/pressure sensors, nanoNMR etc. It is not possible to cover every aspect of microwave plasma CVD grown SCD in a single review article. There are review papers solely discussing, say "NV centre" [235] or "diamond photonics" [253] or "isotope engineering" [215] etc., in recent years. Here, an attempt has been made to provide an

overview of the present scenario of the single crystal diamond research (although leading researchers across the world recently published similar reviews [18, 63, 69] but they do not have free access to the researchers from poorer countries and are also few years older), alongwith its presentday and future applications. Research in this area is going to explode in the coming years [285, 286] and will change the modern civilisation by providing new engineering solutions to the present day impossibilities. The present review paper is an updated status of this field which has not been included in the earlier similar publications. Companies like Microsoft, IBM have started projects aiming to build quntum computers in the next 10-15 years, and the first prototypes of which have already been demonstrated at MIT, USA or Delft University, Netherlands. Parallel computations based on quantum theory, in opposed to classical computation by 0 & 1 only, with the help of tiny SCD qubits (may be smaller than sand grains), will solve problems in no time.

ACKNOWLEDGEMENTS

REFERENCES

[1] Tokuyuki T. Chemical vapor deposition of homoepitaxial diamond films, physica status solidi (a), Special Issue: Selected Topics in Physics and Applications of CVD Diamond 2006; 203: 3324-3357.

[2] Derjaguin BV, Spitsyn BV, Gorodetsky AE, Zakharov AP, Bouilov LL, Aleksenko AE. Structure of autoepitaxial diamond films. J Crystal Growth 1975; 31: 44-48. http://dx.doi.org/10.1016/0022-0248(75)90108-6

[3] Spitsyn BV, Bouilov LL, Derjaguin BV. Vapor growth of diamond on diamond and other surfaces. J Crystal Growth 1981; 52: 219-226. http://dx.doi.org/10.1016/0022-0248(81)90197-4

[4] Mutsukazu K, Yoichiro S, Seiichiro M, Nobuo S. Diamond synthesis from gas phase in microwave plasma. Journal of Crystal Growth 1983; 62: 642-644. http://dx.doi.org/10.1016/0022-0248(83)90411-6

[5] Fedosayev DV, Deryagin BV, Virasavskaja IG. The Crystallization of Diamond, Part I, Moscow: Nauka 1984.

[6] Hiromoto N, Yasuo K, Mutsukazu K, Kazumasa O. X-ray section topographs of a vapour-grown diamond film on a diamond substrate. Thin Solid Films 1987; 151:199-206. http://dx.doi.org/10.1016/0040-6090(87)90233-1

[7] Koji K, Kozo N, Yoshio K, Takefumi H. Synthesis of diamonds by use of microwave plasma chemical-vapor deposition: morphology and growth of diamond films. Phys Rev B 1988; 38: 4067-4084. http://dx.doi.org/10.1103/PhysRevB.38.4067

[8] Yoshikawa M, Ishida H, Shitani A, Murakami IT, Koizumi S, Inuzuka T. study of crystallographic orientations in the diamond film on cubic boron nitride using Raman microprobe. Appl Phys Lett 1990; 57: 428-430. http://dx.doi.org/10.1063/1.103656

[9] Angus John C. Diamond synthesis by chemical vapor deposition: The early years. Diamond & Related Materials 2014; 49: 77-86. http://dx.doi.org/10.1016/j.diamond.2014.08.004

[10] Bachmann Peter K, Dieter L, Hans L. Towards a general concept of diamond chemical vapour deposition Diamond and Related Materials I 1991; 1: 12.

[11] Toyota H, Nomura S, Mukasa S, Yamashita H, Shimo T, Okuda S. A consideration of ternary C-H-O diagram for diamond deposition using microwave in-liquid and gas phase plasma. Diamond & Related Materials 2011; 20: 1255-1258. http://dx.doi.org/10.1016/j.diamond.2011.07.010

[12] Choy KL. Chemical vapour deposition of coatings. Progress in Materials Science 2003; 48: 57-170. http://dx.doi.org/10.1016/S0079-6425(01)00009-3

[13] Jiang X, Klages C-P. Heteroepitaxial diamond growth on (100) silicon. Diamond Relat Mater 1993; 2: 1112-1113. http://dx.doi.org/10.1016/0925-9635(93)90282-7

[14] Jiang X. Textured and Heteroepitaxial CVD Diamond films, Elsevier Inc. 2003; Chapter 1, pp.1-47. ISBN: 0-12-752185-2, ISSN: 0080-8784.

[15] Jiang X, Fryda UM, Jia CL. High quality heteroepitaxial diamond films on silicon: recent progresses. Diamond and Related Materials 2000; 9: 1640-1645. http://dx.doi.org/10.1016/S0925-9635(00)00326-5

[16] Nemanich Robert J, Carlisle John A, Atsushi H, Ken H. CVD diamond-Research, applications, and challenges. MRS Bulletin 2014; 39: 490-494. http://dx.doi.org/10.1557/mrs.2014.97

[17] Norio T. Homoepitaxial Diamond Growth by Plasma-Enhanced Chemical Vapor Deposition, Chapter 1, pp.1-29, Novel Aspects of Diamond, Springer International Publishing Switzerland, 2015, N. Yang ed, Topics in Applied Physics 121.

[18] Matthias S, Jes A, Shinichi S, Jean-Charles A, Naoji F. CVD Diamond-Research, Applications, and Challenges Large-area high-quality single crystal diamond. MRS Bulletin 2014; 39: 504-510. http://dx.doi.org/10.1557/mrs.2014.96

[19] Khmelnitskiy RA. Prospects for the synthesis of large single-crystal diamonds. Physics-Uspekhi 2015; 58: 134-149. http://dx.doi.org/10.3367/UFNe.0185.201502b.0143

[20] Bogdan G, Corte K. De, Deferme W, Haenen K, Nesládek M. Thick single crystal CVD diamond prepared from CH4-rich mixtures. Phys Status Solidi A Appl Res 2006; 203: 3063. http://dx.doi.org/10.1002/pssa.200671128

[21] Michael S, Knut P. A review of diamond synthesis by CVD processes. Diamond & Related Materials 2011; 20: 1287-1301. http://dx.doi.org/10.1016/j.diamond.2011.08.005

[22] Ding Ming Q, Lili L, Jinjun F. A study of high-quality freestanding diamond films grown by MPCVD. Applied Surface Science 2012; 258: 5987-5991. http://dx.doi.org/10.1016/j.apsusc.2012.02.025

[23] Weng J, Xiong LW, Wang JH, Dai SY, Man WD, Liu F. Investigation of depositing large area uniform diamond films in multi-mode MPCVD chamber. Diamond & Related Materials 2012; 30: 15-19. http://dx.doi.org/10.1016/j.diamond.2012.09.007

[24] Kromka A, Babchenko O, Izak T, Hruska K, Rezek B. Linear antenna microwave plasma CVD deposition of diamond films over large areas. Vacuum 2012; 86: 776-779. http://dx.doi.org/10.1016/j.vacuum.2011.07.008

[25] Nagatsu M, Makino M, Tang M, Sugai H. Diagnostics of plasma ball formed in high pressure microwave plasma for diamond film synthesis. Diamond and Related Materials 2002; 11: 562-566. http://dx.doi.org/10.1016/S0925-9635(01)00632-X

[26] Wei JJ, Liu JL, Chen LX, Hei LF, Lv FX, Li ChM. Amination of diamond film by ammonia microwave plasma treatment. Diamond & Related Materials 2015; 54: 34-38. http://dx.doi.org/10.1016/j.diamond.2014.10.014

[27] Marian V, Marian V, Oleg B, Tibor I, Miroslav M, Marián M, Alexander K. Structural and electrical characterization of diamond films deposited in nitrogen/oxygen containing gas mixture by linear antennamicrowave CVD process. Applied Surface Science 2014; 312: 226-230. http://dx.doi.org/10.1016/j.apsusc.2014.05.176

[28] Armando N, Michael F. Kinetic Monte Carlo simulations of CVD diamond growth-Interlay among growth, etching, and migration. Diamond & Related Materials 2005; 14: 1630-1646. http://dx.doi.org/10.1016/j.diamond.2005.05.009

[29] Shyam K, Manoj J, Reeti B, Divyash P, Misra DS, Das Gupta K, Varma R. Growth of Diamond by MPCVD Process. Proceedings of the DAE Symp on Nucl Phys 2013; 58: 920-921.

[30] Tang CJ, Fernandes AJS, Marco G, Leitao JP, Pereira S, Jiang XF, Pinto JL, Ye H. High rate growth of nanocrystalline diamond films using high microwave power and pure nitrogen/methane/hydrogen plasma. Vacuum 2015; xxx: 1-5.

[31] Weng J, Wang JH, Dai SY, Xiong LW, Man WD, Liu F. Preparation of diamond films with controllable surface morphology, orientation and quality in an overmoded microwave plasma CVD chamber. Applied Surface Science 2013; 276: 529- 534. http://dx.doi.org/10.1016/j.apsusc.2013.03.128

[32] An K, Yu SW, Li XJ, Shen YY, Zhou B, Zhang GJ, Liu XP. Microwave plasma reactor with conical-reflector for diamond Deposition. Vacuum 2015; 117: 112-120.
http://dx.doi.org/10.1016/j.vacuum.2015.04.023

[33] Watanabe H, Takeuchi D, Yamanaka S, Okushi H, Kajimura K, Sekiguchi T. Homoepitaxial diamond film with an atomically flat surface over a large area. Diamond Relat Mater 1999; 8: 1272-1276.
http://dx.doi.org/10.1016/S0925-9635(99)00126-0

[34] Chayahara A, Mokuno Y, Horino Y, Takasu Y, Kato H, Yoshikawa H, Fujimori N. The effect of nitrogen addition during high-rate homoepitaxial growth of diamond by microwave plasma CVD. Diamond Relat Mater 2004; 13: 1954-1956.
http://dx.doi.org/10.1016/j.diamond.2004.07.007

[35] Bauer Th, Schreck M, Stritzker B. Homoepitaxial diamond layers on off-axis Ib HPHT substrates: Growth of thick films and characterisation by high-resolution X-ray diffraction. Diamond Relat Mater 2006; 15: 472-478.
http://dx.doi.org/10.1016/j.diamond.2005.09.028

[36] Enckevort WJP, van Janssen G, Schermer JJ, Giling LJ. Step-related growth phenomena on exact and misoriented {001} surfaces of CVD-grown single-crystal diamonds. Diamond Relat Mater 1995; 4: 250-255.
http://dx.doi.org/10.1016/0925-9635(94)05201-8

[37] Hickey DP, Jones KS, Elliman RG. Amorphization and graphitization of single-crystal diamond A transmission electron microscopy study. Diamond & Related Materials 2009; 18: 1353-1359.
http://dx.doi.org/10.1016/j.diamond.2009.08.012

[38] Alastair S, Igor A, Steven P, Butler James E. Controlled synthesis of high quality micro/nano-diamonds by microwave plasma chemical vapor deposition. Diamond & Related Materials 2009; 18: 51-55.
http://dx.doi.org/10.1016/j.diamond.2008.09.020

[39] Gu Yajun J, Lu Grotjohn T, Schuelke T, Asmussen J. Microwave plasma reactor design for high pressure and high power density diamond synthesis. Diamond & Related Materials 2012; 24: 210-214.
http://dx.doi.org/10.1016/j.diamond.2012.01.026

[40] Grotjohn T, Liske R, Hassouni K, Asmussen J. Scaling behavior of microwave reactors and discharge size for diamond deposition. Diamond & Related Materials 2005; 14: 288- 291.
http://dx.doi.org/10.1016/j.diamond.2004.12.017

[41] Kuo-Ping K, Jes A. An experimental study of high pressure synthesis of a microwave cavity plasma reactor. Diamond and Related Materials 1997; 6: 1097- 1105.
http://dx.doi.org/10.1016/S0925-9635(97)00018-6

[42] Grotjohn TA, Asmussen J, Sivagnaname J, Story D, Vikharev AL, Gorbachev A, Kolysko A. Electron density in moderate pressure diamond deposition discharges. Diamond and Related Materials 2000; 9: 322-327.
http://dx.doi.org/10.1016/S0925-9635(99)00211-3

[43] Hemawan KW, Grotjohn TA, Reinhard DK, Asmussen J. Improved microwave plasma cavity reactor for diamond synthesis at high-pressure and high power density. Diamond & Related Materials 2010; 19: 1446-1452.
http://dx.doi.org/10.1016/j.diamond.2010.07.005

[44] Lu J, Gu Y, Grotjohn TA, Schuelke T, Asmussen J. Experimentally defining the safe and efficient, high pressure microwave plasma assisted CVD operating regime for single crystal diamond synthesis. Diamond & Related Materials 2013; 37: 17-28.
http://dx.doi.org/10.1016/j.diamond.2013.04.007

[45] Jing L. Single Crystal Microwave Plasma Assisted Chemical Vapor Diamond Synthesis at High Pressures and High Power Densities, PhD Thesis, Electrical Engineering, Michigan State University 2013.

[46] Hideaki Y, Akiyoshi C, Yoshiaki M, Nobuteru T, Shin-ichi S, Naoji F. Developments of elemental technologies to produce inch-size single-crystal diamond wafers. Diamond & Related Materials 2011; 20: 616-619.
http://dx.doi.org/10.1016/j.diamond.2011.01.001

[47] Hideaki Y, Akiyoshi C, Yoshiaki M, Shinichi S. Numerical microwave plasma discharge study for the growth of large single-crystal diamond. Diamond & Related Materials 2015; 54: 9-14.
http://dx.doi.org/10.1016/j.diamond.2014.11.005

[48] Akoshi C, Yoshiaki M, Nobuteru T, Hideaki Y. Development of single crystalline diamond wafers - Enlargement of crystal size by microwave plasma CVD and wafer fabrication technology. Synthesiology 2010; 3: 272-280.
http://dx.doi.org/10.5571/synth.3.272

[49] Hideaki Y, Akiyoshi C, Yoshiaki M, Shin-ichi S. Simulation with an improved plasma model utilized to design a new structure of microwave plasma discharge for chemical vapour deposition of diamond crystals. Diamond & Related Materials 2008; 17: 494-497.
http://dx.doi.org/10.1016/j.diamond.2007.08.036

[50] Chayahara A, Mokuno Y, Horino Y, Takasu Y, Kato H, Yoshikawa H, Fujimori N. The effect of nitrogen addition during high-rate homoepitaxial growth of diamond by microwave plasma CVD. Diamond & Related Materials 2004; 13: 1954-1958.
http://dx.doi.org/10.1016/j.diamond.2004.07.007

[51] Hideaki Y, Akiyoshi C, Yoshiaki M, Nobuteru T, Shin-ichi S. Uniform growth and repeatable fabrication of inch-sized wafers of a single-crystal diamond. Diamond & Related Materials 2013; 33: 27-31.
http://dx.doi.org/10.1016/j.diamond.2012.12.012

[52] Mokuno Y, Chayahara A, Soda Y, Horino Y, Fujimori N. Synthesizing single-crystal diamond by repetition of high rate homoepitaxial growth by microwave plasma CVD. Diamond & Related Materials 2005; 14: 1743-1746.
http://dx.doi.org/10.1016/j.diamond.2005.09.020

[53] Yamada H, Chayahara A, Mokuno Y, Kato Y, Shikata S. Effects of crystallographic orientation on the homoepitaxial overgrowth on tiled single crystal diamond clones. Diamond & Related Materials 2015; 57: 17-21.
http://dx.doi.org/10.1016/j.diamond.2015.01.007

[54] Mokuno Y, Chayahara A, Yamada H, Tsubouchi N. Improving purity and size of single-crystal diamond plates produced by high-rate CVD growth and lift-off process using ion implantation. Diamond & Related Materials 2009; 18: 1258-1261.
http://dx.doi.org/10.1016/j.diamond.2009.04.005

[55] Tsubouchi N, Umezawa H, Mokuno Y, Chayahara A, Shikata S. Lattice structure of a freestanding nitrogen doped large single crystal diamond plate fabricated using the lift-off process: X-ray diffraction studies. Diamond & Related Materials 2012; 25: 119-123.
http://dx.doi.org/10.1016/j.diamond.2012.01.007

[56] Yamada H, Chayahara A, Umezawa H, Tsubouchi N, Mokuno Y, Shikata S. Fabrication and fundamental characterizations of tiled clones of single-crystal diamond with 1-inch size. Diamond & Related Materials 2012; 24: 29-33.
http://dx.doi.org/10.1016/j.diamond.2011.09.007

[57] Silva F, Achard J, Bonnin X, Brinza O, Michau A, Secroun A, Corte K. De, Felton S, Newton M, Gicquel A. Single crystal CVD diamond growth strategy by the use of a 3D geometrical model: Growth on (113) oriented substrates. Diamond & Related Materials 2008; 17: 1067-1075.
http://dx.doi.org/10.1016/j.diamond.2008.01.006

[58] Silva F, Bonnin X, Achard J, Brinza O, Michau A, Gicquel A. Geometric modeling of homoepitaxial CVD diamond growth: I. The {1 0 0}{1 1 1}{1 1 0}{1 1 3} system. Journal of Crystal Growth 2008; 310: 187-203.
http://dx.doi.org/10.1016/j.jcrysgro.2007.09.044

[59] Silva F, Achard J, Brinza O, Bonnin X, Hassouni K, Anthonis A, Corte K. De, Barjon J. High quality, large surface area, homoepitaxial MPACVD diamond growth. Diamond & Related Materials 2009; 18: 683-697.
http://dx.doi.org/10.1016/j.diamond.2009.01.038

[60] Gicquel A, Hassouni K, Farhat S, Breton Y, Scott CD, Lefebvre M, Pealat M. Spectroscopic analysis and chemical kinetics modelling of a diamond deposition plasma reactor. Diamond and Related Materials 1994; 3: 581-586.
http://dx.doi.org/10.1016/0925-9635(94)90229-1

[61] Gicquel A, Derkaoui N, Rond C, Benedic F, Cicala G, Moneger D, Hassouni K. Quantitative analysis of diamond deposition reactor efficiency. Chemical Physics 2012; 398: 239-247.
http://dx.doi.org/10.1016/j.chemphys.2011.08.022

[62] Silva F, Bonnin X, Scharpf J, Alberto P. Microwave analysis of PACVD diamond deposition reactor based on electromagnetic modelling. Diamond & Related Materials 2010; 19: 397-403.
http://dx.doi.org/10.1016/j.diamond.2009.10.032

[63] Tallaire A, Achard J, Silva F, Brinza O, Gicquel A. Growth of large size diamond single crystals by plasma assisted chemical vapour deposition: Recent achievements and remaining challenges. C R Physique 2013; 14: 169-184.
http://dx.doi.org/10.1016/j.crhy.2012.10.008

[64] Tallaire A, Achard J, Boussadi A, Brinza O, Gicquel A, Kupriyanov IN, Palyanov YN, Sakr G, Barjon J. High quality thick CVD diamond films homoepitaxially grown on (111)-oriented substrates. Diamond and Related Materials 2014; 41: 34-40.
http://dx.doi.org/10.1016/j.diamond.2013.11.002

[65] Lesik M, Plays T, Tallaire A, Achard J, Brinza O, William L, Chipaux M, Toraille L, Debuisschert T, Gicquel A, Rocha JF, Jacques V.

Preferential orientation of NV defects in CVD diamond films grown on (113)-oriented substrates. Diamond & Related Materials 2015; 56: 47-53.
http://dx.doi.org/10.1016/j.diamond.2015.05.003

[66] Naamoun M, Tallaire A, Silva F, Achard J, Doppelt P, and Gicquel A. Etch-pit formation mechanism induced on HPHT and CVD diamond single crystals by H2/O2 plasma etching treatment. Phys Status Solidi A 2012; 209: 1715-1720.
http://dx.doi.org/10.1002/pssa.201200069

[67] Chavanne A, Barjon J, Vilquin B, Arabski J, Arnault JC. Surface investigations on different nucleation pathways for diamond heteroepitaxial growth on iridium. Diamond & Related Materials 2012; 22: 52-58.
http://dx.doi.org/10.1016/j.diamond.2011.12.005

[68] Tallaire A, Collins A.T, Charles D, Achard J, Sussmann R, Gicquel A, Newton ME, Edmonds AM, Cruddace RJ. Characterisation of high-quality thick single-crystal diamond grown by CVD with a low nitrogen addition. Diamond & Related Materials 2006; 15: 1700-1707.
http://dx.doi.org/10.1016/j.diamond.2006.02.005

[69] Liang Q, Yan C-S, Meng Y, Lai J, Krasnicki S, Mao H-K, Hemley RJ. Recent advances in high-growth rate single-crystal CVD diamond. Diamond & Related Materials 2009; 18: 698-703.
http://dx.doi.org/10.1016/j.diamond.2008.12.002

[70] Muchnikov AB, Vikharev AL, Gorbachev AM, Radishev DB. Comparative study of homoepitaxial single crystal diamond growth at continuous and pulsed mode of MPACVD reactor operation. Diamond & Related Materials 2011; 20: 1225-1228.
http://dx.doi.org/10.1016/j.diamond.2011.06.030

[71] Muchnikov AB, Vikharev AL, Gorbachev AM, Radishev DB, Blank VD, Terentiev SA. Homoepitaxial single crystal diamond growth at different gas pressures and MPACVD reactor configurations. Diamond & Related Materials 2010; 19: 432-436.
http://dx.doi.org/10.1016/j.diamond.2009.11.012

[72] Ivanov OA, Muchnikov AB, Chernov VV, Bogdanov SA, Vikharev AL, Butler JE. Experimental study of hydrogen plasma etching of (1 0 0) single crystal diamond in a MPACVD reactor. Materials Letters 2015; 151: 115-118.
http://dx.doi.org/10.1016/j.matlet.2015.03.073

[73] Bogatskiy A, Butler JE. A geometric model of growth for cubic crystals: Diamond. Diamond & Related Materials 2015; 53: 58-65.
http://dx.doi.org/10.1016/j.diamond.2014.12.010

[74] Muchnikov AB, Vikharev AL, Gorbachev AM, Radishev DB. Comparative study of homoepitaxial single crystal diamond growth at continuous and pulsed mode of MPACVD reactor operation. Diamond & Related Materials 2011; 20: 1225-1228.
http://dx.doi.org/10.1016/j.diamond.2011.06.030

[75] Li Xiao J, Zheng Shun Q, Zhao Bao R, Zhang Xi W, Tang Wei Z. Design and Numerical Simulation of Novel Reentrant Microwave Cavity. Physics Procedia 2011; 22: 101-106.
http://dx.doi.org/10.1016/j.phpro.2011.11.016

[76] Su JJ, Li YF, Li XL, Yao PL, Liu YQ, Ding MH, Tang WZ. A novel microwave plasma reactor with a unique structure for chemical vapor deposition of diamond films. Diamond & Related Materials 2014; 42: 28-32.
http://dx.doi.org/10.1016/j.diamond.2013.12.001

[77] Su JJ, Li YF, Ding MH, Li XL, Liu YQ, Wang G, Tang WZ. A dome-shaped cavity type microwave plasma chemical vapour deposition reactor for diamond films deposition. Vacuum 2014; 107: 51-55.
http://dx.doi.org/10.1016/j.vacuum.2014.04.002

[78] Li YF, Su JJ, Liu YQ, Ding MH, Li XL, Wang G, Yao PL, Tang WZ. Design of a new TM021 mode cavity type MPCVD reactor for diamond film deposition. Diamond & Related Materials 2014; 44: 88-94.
http://dx.doi.org/10.1016/j.diamond.2014.02.010

[79] Li YF, Su JJ, Liu YQ, Ding MH, Wang G, Tang WZ. A circumferential antenna ellipsoidal cavity type MPCVD reactor developed for diamond film deposition. Diamond & Related Materials 2015; 51: 24-29.
http://dx.doi.org/10.1016/j.diamond.2014.11.004

[80] Li XJ, Tang WZ, Wang FY, Li CM, Hei LF, Lu FX. N.A compact ellipsoidal cavity type microwave plasma reactor for diamond film deposition. Diamond & Related Materials 2011; 20: 374-379.
http://dx.doi.org/10.1016/j.diamond.2011.01.025

[81] Li XJ, Tang WZ, Yu SW, Zhang SK, Chen GC, Lu FX. Design of novel plasma reactor for diamond film deposition. Diamond & Related Materials 2011; 20: 480-484.
http://dx.doi.org/10.1016/j.diamond.2011.01.046

[82] Weng J, Xiong LW, Wang JH, Dai SY, Man WD, Liu F. Investigation of depositing large area uniform diamond films in multi-mode MPCVD chamber. Diamond & Related Materials 2012; 30: 15-19.
http://dx.doi.org/10.1016/j.diamond.2012.09.007

[83] Mankelevich YuA, May PW. New insights into the mechanism of CVD diamond growth: Single crystal diamond in MW PECVD reactors. Diamond & Related Materials 2008; 17: 1021-1028.
http://dx.doi.org/10.1016/j.diamond.2008.03.022

[84] Rodgers WJ, May PW, Allan NL, Harvey JN. Three-dimensional kinetic Monte Carlo simulations of diamond chemical vapor deposition. Journal of Chemical Physics 2015; 142: 214707.
http://dx.doi.org/10.1063/1.4921540

[85] Mankelevich Yuri. A, Ashfold Michael N.R, Ma Jie. Plasma-chemical processes in microwave plasma-enhanced chemical vapor deposition reactors operating with C/H/Ar gas mixtures. Journal of Applied Physics 2008; 104: 113304-113314.
http://dx.doi.org/10.1063/1.3035850

[86] Cheesman A, Smith JA, Ashfold MNR, Langford N, Wright S, Duxbury G. Application of a quantum cascade laser for time-resolved, in situ probing of CH4/H2 and C2H2/H2 gas mixtures during microwave plasma enhanced chemical vapor deposition of diamond. Journal of Physical Chemistry A 2006; 110: 2821-2828.
http://dx.doi.org/10.1021/jp056622u

[87] Ma Jie, Richley James. C, Ashfold Michael NR, Yuri A. Mankelevich. Probing the plasma chemistry in a microwave reactor used for diamond chemical vapor deposition by cavity ring down spectroscopy. Journal of Applied Physics 2008; 104: 103305.
http://dx.doi.org/10.1063/1.3021095

[88] Butler JE, Mankelevich YA, Cheesman A, Ma Jie, Ashfold MNR. Understanding the chemical vapor deposition of diamond: recent progress. Journal of Physics: Condensed Matter 2009; 21: 364201-364221.
http://dx.doi.org/10.1088/0953-8984/21/36/364201

[89] Martineau PM, Gaukroger MP, Guy KB, Lawson SC, Twitchen DJ, Friel I, Hansen JO, Summerton GC, Addison TPG, Burns R. High crystalline quality single crystal CVD diamond. Journal of Physics: Condensed Matter 2009; 21: 364205.
http://dx.doi.org/10.1088/0953-8984/21/36/364205

[90] Isberg J, Hammersberg J, Johansson E, Wikström T, Twitchen DJ, Whitehead AJ, Coe SE, Scarsbrook GA. High Carrier Mobility in Single-Crystal Plasma-Deposited Diamond. Science 2002; 297: 1670.
http://dx.doi.org/10.1126/science.1074374

[91] Scarsbrook GA, Wilman JJ, Dodson JM, Brandon JR, Coe SE, Wort CJH. A microwave plasma reactor for manufacturing synthetic diamond material. United States patent US20140048016 A1. 2014 Feb.

[92] Chen GC, Li B, Yan ZQ, Lu FX. Single crystalline diamond grown by repositioning substrate in DC arcjet plasma enhanced chemical vapor deposition. Diamond & Related Materials 2012; 21: 83-87.
http://dx.doi.org/10.1016/j.diamond.2011.10.009

[93] Liu J, Hei LF, Song JH, Li CM, Tang WZ, Chen GC, Lu FX. High-rate homoepitaxial growth of CVD single crystal diamond by dc arc plasma jet at blow-down (open cycle) mode. Diamond & Related Materials 2014; 46: 42-51.
http://dx.doi.org/10.1016/j.diamond.2014.04.008

[94] Hei LF, Liu J, Li CM, Song JH, Tang WZ, Lu FX. Fabrication and characterizations of large homoepitaxial single crystal diamond grown by DC arc plasma jet CVD. Diamond & Related Materials 2012; 30: 77-84.
http://dx.doi.org/10.1016/j.diamond.2012.10.002

[95] Chiu K-A, Wu P-H, Peng C-Y, Tian J-S, Chang L. Homoepitaxial growth and stress analysis of (111) diamond film with embedded gold islands. Vacuum 2015; 118: 104-108.
http://dx.doi.org/10.1016/j.vacuum.2015.01.013

[96] Chiu K-A, Tian J-S, Wu Y-H, Peng C-Y, Chang L. Stress reduction of (111) homoepitaxial diamond films on nickel-coated substrate. Surface & Coatings Technology 2014; 259: 358-362.
http://dx.doi.org/10.1016/j.surfcoat.2014.03.012

[97] Naamoun M, Tallaire A, Doppelt P, Gicquel A, Legros M, Barjon J, Achard J. Reduction of dislocation densities in single crystal CVD diamond by using self-assembled metallic masks. Diamond & Related Materials 2015; 58: 62-68.
http://dx.doi.org/10.1016/j.diamond.2015.06.012

[98] Regmi M, More K, Eres G. A narrow biasing window for high density diamond nucleation on Ir/YSZ/Si(100) using microwave plasma chemical vapor deposition. Diamond & Related Materials 2012; 23: 28-33.
http://dx.doi.org/10.1016/j.diamond.2012.01.008

[99]   Gsell S, Schreck M, Benstetter G, Lodermeier E, Stritzker B. Combined AFM-SEM study of the diamond nucleation layer on Ir(001). Diamond & Related Materials 2007; 16: 665-670.
http://dx.doi.org/10.1016/j.diamond.2006.11.091

[100]   Gsell S, Berner S, Brugger T, Schreck M, Brescia R, Fischer M, Greber T, Osterwalder J, Stritzker B. Comparative electron diffraction study of the diamond nucleation layer on Ir(001). Diamond & Related Materials 2008; 17: 1029-1034.
http://dx.doi.org/10.1016/j.diamond.2008.02.040

[101]   Brescia R, Schreck M, Gsell S, Fischer M, Stritzker B. Transmission electron microscopy study of the very early stages of diamond growth on iridium. Diamond & Related Materials 2008; 17: 1045-1050.
http://dx.doi.org/10.1016/j.diamond.2008.01.115

[102]   Schreck M, Gsell S, Brescia R, Fischer M, Bernhard P, Prunici P, Hess P, Stritzker B. Diamond nucleation on iridium: Local variations of structure and density within the BEN layer. Diamond & Related Materials 2009; 19: 107-112.
http://dx.doi.org/10.1016/j.diamond.2008.08.013

[103]   Gsell S, Fischer M, Bauer T, Schreck M, Stritzker B. Yttria-stabilized zirconia films of different composition as buffer layers for the deposition of epitaxial diamond/Ir layers on Si(001). Diamond Relat Mater 2006; 15: 479.
http://dx.doi.org/10.1016/j.diamond.2005.10.041

[104]   Fischer M, Gsell S, Schreck M, Brescia R, Stritzker B. Preparation of 4-inch Ir/YSZ/Si(001) substrates for the large-area deposition of single-crystal diamond. Diamond & Related Materials 2008; 17: 1035-1038.
http://dx.doi.org/10.1016/j.diamond.2008.02.028

[105]   Brescia R, Schreck M, Michler J, Gsell S, Stritzker B. Interaction of small diamond islands on iridium: A finite element simulation study. Diamond & Related Materials 2007; 16: 705-710.
http://dx.doi.org/10.1016/j.diamond.2007.01.029

[106]   Su Y, Li HD, Cheng SH, Zhang Q, Wang QL, Lv XY, Zou GT, Pei XQ, Xie JG. Effect of N_2O on high-rate homoepitaxial growth of CVD single crystal diamonds. Journal of Crystal Growth 2012; 351: 51-55.
http://dx.doi.org/10.1016/j.jcrysgro.2012.03.041

[107]   Zhang Q, Li HD, Cheng SH, Wang QL, Li LA, Lv XY, Zou GT. The effect of CO_2 on the high-rate homoepitaxial growth of CVD single crystal diamonds. Diamond & Related Materials 2011; 20: 496-500.
http://dx.doi.org/10.1016/j.diamond.2011.02.001

[108]   Ohmagari S, Yamada H, Umezawa H, Chayahara A, Teraji T, Shikata S. Characterization of free-standing single-crystal diamond prepared by hot-filament chemical vapor deposition. Diamond & Related Materials 2014; 48: 19-23.
http://dx.doi.org/10.1016/j.diamond.2014.06.001

[109]   Chu CJ, Hauge RH, Margrave JL, D'Evelyn MP. Growth kinetics of (100), (110), and (111) homoepitaxial diamond films. Appl Phys Lett 1992; 61: 1393.
http://dx.doi.org/10.1063/1.107548

[110]   Avigal Y, C. Saguy Uzan-, Kalish R, Lereah Y. Diamond homoepitaxy by hot-filament chemical vapor deposition. Diamond Relat Mater 1993; 2: 462.
http://dx.doi.org/10.1016/0925-9635(93)90101-7

[111]   Stammler M, Eisenbeiß H, Ristein J, Neubauer J, Göbbels M, Ley L. Growth of high-quality homoepitaxial diamond films by HF-CVD. Diamond Relat Mater 2002; 11: 504.
http://dx.doi.org/10.1016/S0925-9635(01)00627-6

[112]   http://www.seocal.com/pdf/Data_Sheet_3.pdf, last accessed on 16th October, 2015.

[113]   http://www.owwz.de/fileadmin/Veranstaltungen/Nanoforum_Tomsk_2010/Nanomaterials/6.pdf, last accessed on 16th October, 2015.

[114]   Cheng C-L, Chang H-C, Lin J-C, Song K-J, Wang JK. Direct observation of hydrogen etching anisotropy on diamond single crystal surfaces. Phys Rev Lett 1997; 78(19): 3713-3716.
http://dx.doi.org/10.1103/PhysRevLett.78.3713

[115]   Yamada H, Chayahara A, Mokuno Y, Shikata S. Model of reactive microwave plasma discharge for growth of single-crystal diamond. Jpn J Appl Phys 2011; 50(1S1): 01AB02.

[116]   Yamada H. Numerical simulations to study growth of single-crystal diamond by using microwave plasma chemical vapor deposition with reactive (H, C, N) species. Jpn J Appl Phys 2012; 51(9R): 090105.
http://dx.doi.org/10.7567/JJAP.51.090105

[117]   Achard J, Silva F, Tallaire A, Bonnin X, Lomvardi G, Hassouni K, Gicquel A. High quality MPACVD diamond single crystal growth: high microwave power density regime. J Phys 2007; D 40(20): 6175-6188.

[118]   Zhou H, Watanabe J, Miyake M, Ogino A, Nagatsu M, Zhan R. Optical and mass spectroscopy measurements of Ar/CH4/H2

microwave plasma for nano-crystalline diamond film deposition. Diam Relat Mater 2007; 16(4-7): 675-678.
http://dx.doi.org/10.1016/j.diamond.2006.11.074

[119]   Kato Y, Umezawa H, Shikata S, Touge M. Effect of an ultraflat substrate on the epitaxial growth of chemical-vapor-deposited diamond. Appl Phys Express 2013; 6(2): 025506.
http://dx.doi.org/10.7567/APEX.6.025506

[120]   Yang N, Zong W, Li Z, Sun T. Wear process of single crystal diamond affected by sliding velocity and contact pressure in mechanical polishing. Diamond & Related Materials 2015; 58: 46-53.
http://dx.doi.org/10.1016/j.diamond.2015.06.004

[121]   Pinto H, Jones R. Theory of the birefringence due to dislocations in single crystal CVD diamond. J Phys Condens Matter 2009; 21: 364220.
http://dx.doi.org/10.1088/0953-8984/21/36/364220

[122]   McNamara D, Alveen P, Damm S, Carolan D, Rice JH, Murphy N, Ivankovic A. A Raman spectroscopy investigation into the influence of thermal treatments on the residual stress of polycrystalline diamond. Int Journal of Refractory Metals and Hard Materials 2015; 52: 114-122.
http://dx.doi.org/10.1016/j.ijrmhm.2015.04.025

[123]   El-Diasty F. Coherent anti-Stokes Raman scattering: Spectroscopy and microscopy. Vibrational Spectroscopy 2011; 55: 1-37.
http://dx.doi.org/10.1016/j.vibspec.2010.09.008

[124]   Kato Y, Umezawa H, Shikata S, Teraji T. Local stress distribution of dislocations in homoepitaxial chemical vapor deposite single-crystal diamond. Diamond & Related Materials 2012; 23: 109-111.
http://dx.doi.org/10.1016/j.diamond.2012.01.024

[125]   Tallaire A, Achard J, Brinza O, Mille V, Naamoun M, Silva F, Gicquel A. Growth strategy for controlling dislocation densities and crystal morphologies of single crystal diamond by using pyramidal-shape substrates. Diamond & Related Materials 2013; 33: 71-77.
http://dx.doi.org/10.1016/j.diamond.2013.01.006

[126]   Achatz P, Omnès F, Ortéga L, Marcenat C, Vacík J, Hnatowicz V, Köster U, Jomard F, Bustarret E. Isotopic substitution of boron and carbon in superconducting diamond epilayers grown by MPCVD. Diamond & Related Materials 2010; 19: 814-817.
http://dx.doi.org/10.1016/j.diamond.2010.01.052

[127]   Ramamurti R, Becker M, Schuelke T, Grotjohn TA, Reinhard DK, Asmussen J. Deposition of thick boron-doped homoepitaxial single crystal diamond by microwave plasma chemical vapor deposition. Diamond & Related Materials 2009; 18: 704-706.
http://dx.doi.org/10.1016/j.diamond.2009.01.031

[128]   Maida O, Tada S, Ito T. High growth rate deposition of phosphorus-doped homoepitaxial (001) diamond films for deep-ultraviolet light emitting device. Thin Solid Films 2014; 557: 227-230.
http://dx.doi.org/10.1016/j.tsf.2013.08.114

[129]   Maida O, Tada S, Nishio H, Ito T. Substrate temperature optimization for heavily-phosphorus-doped diamond films grown on vicinal (001) surfaces using high-power-density microwave-plasma chemical-vapor-deposition. Journal of Crystal Growth 2015; 424: 33-37.
http://dx.doi.org/10.1016/j.jcrysgro.2015.04.037

[130]   Ratnikova AK, Dukhnovsky MP, Fedorov YuYu, Zemlyakov VE, Muchnikov AB, Vikharev AL, Gorbachev AM, Radishev DB, Altukhov AA, Mitenkin AV. Homoepitaxial single crystal diamond grown on natural diamond seeds (type IIa) with boron-implanted layer demonstrating the highest mobility of 1150 cm2/V.s at 300 K for ion-implanted diamond. Diamond & Related Materials 2011; 20: 1243-1245.
http://dx.doi.org/10.1016/j.diamond.2011.07.007

[131]   Issaoui R, Achard J, Silva F, Tallaire A, Tardieu A, Gicquel A, Inault MAP, Jomard F. Growth of thick heavily boron-doped diamond single crystals: Effect of microwave power density. Applied Physics Letters 2010; 97: 182101.
http://dx.doi.org/10.1063/1.3511449

[132]   Tapper RJ. Diamond detectors in particle physics. Rep Prog Phys 2000; 63: 1273-1316.
http://dx.doi.org/10.1088/0034-4885/63/8/203

[133]   Meier D. CVD Diamond Sensors for Particle Detection and Tracking, PhD Dissertation, CERN, Geneva, January 1999.

[134]   Oh A. Particle detection with CVD diamond, PhD Thesis, Institute for Experimental Physics, University of Hamburg 1999.

[135]   Misra DS, Palnitkar U, Tyagi PK, Singh MK, Titus E, Avasthi DK, Vasa P, Ayyub P. Melting and defect generation in chemical vapor deposited diamond due to irradiation with 100 MeV Au+ and Ag+ ions. Thin Solid Films 2006; 503: 121-126.
http://dx.doi.org/10.1016/j.tsf.2005.11.029

[136] Pomorski M, Berdermann E, Boer W. de, Furgeri A, Sander C, Morse J. Charge transport properties of single crystal CVD-diamond particle detectors. Diamond & Related Materials 2007; 16: 1066-1069.
http://dx.doi.org/10.1016/j.diamond.2006.11.016

[137] Schirru F, Chokheli D, Kiš M. Thin single crystal diamond detectors for alpha particle detection. Diamond and Related Materials 2014; 49: 96-102.
http://dx.doi.org/10.1016/j.diamond.2014.08.001

[138] Bartz E, Doroshenko J, Halyo, Harrop B, Hits DA, Marlow D, Pereraay L, Schnetzea S, Stone R. The PLT: A Luminosity Monitor for CMS Based on Single-Crystal Diamond Pixel Sensors. Nuclear Physics B - Proceedings Supplements 2009; 197: 171-174.
http://dx.doi.org/10.1016/j.nuclphysbps.2009.10.060

[139] Tsubota M, Kaneko JH, Miyazaki D, Shimaoka T, Ueno K, Tadokoro T, Chayahara A, Watanabe H, Kato Y, Shikata S, Kuwabara H. High-temperature characteristics of charge collection efficiency using single CVD diamond detectors. Nuclear Instruments and Methods in Physics Research A 2015; 789: 50-56.
http://dx.doi.org/10.1016/j.nima.2015.04.002

[140] Carballo Maria Elena Castro, Zeuthen DESY. Application of single crystal diamonds (sCVD) as beam conditions monitors at LHC, BI Seminar CERN, November 2012.

[141] Bachmair F, Bäni L, Bergonzo P, Caylar B, Forcolin G, Haughton I, Hits D, Kass H, Kagan L, Li R, Ohc A, Phan S, Pomorski M, Smith DS, Tyzhnevyi V, Wallny R, Whitehead D. A 3D diamond detector for particle tracking. Nuclear Instruments and Methods in Physics Research A 2015; 786: 97-104.
http://dx.doi.org/10.1016/j.nima.2015.03.033

[142] Slide presentation by Smith J. M. Diamond based particle detection, CMS, CERN, 2014.

[143] Bohon J, Muller E, Smedley J. Development of diamond-based X-ray detection for high-flux beamline diagnostics. J Synchrotron Rad 2010; 17: 711-718.
http://dx.doi.org/10.1107/S0909049510031420

[144] Sato Y, Shimaoka T, Kaneko JH, Murakami H, Isobe M, Osakabe M, Tsubota M, Ochiai K, Chayahara A, Umezawa H, Shikata S. Radiation hardness of a single crystal CVD diamond detector for MeV energy protons. Nuclear Instruments and Methods in Physics Research A 2015; 784:147-150.
http://dx.doi.org/10.1016/j.nima.2014.12.036

[145] Cazzaniga C, Sundén E. Andersson, Binda F, Croci G, Ericsson G, Giacomelli L, Gorini G, Griesmayer E, Grosso G, Kaveney G, Nocente M, Cippo E. Perelli, Rebai M, Syme B, Tardocchi M and JET-EFDA Contributors. Single crystal diamond detector measurements of deuterium-deuterium and deuterium-tritium neutrons in Joint European Torus fusion plasmas. Review of Scientific Instruments 2014; 85: 043506.
http://dx.doi.org/10.1063/1.4870584

[146] Pietraszko J, Fabbietti L, Koenig W. Diamonds as timing detectors for MIP: The HADES proton-beam monitor and start detectors, Nuclear Instruments and Methods in Physics Research section A: Accelerometers, Spectrometers. Detectors and Associated Instruments 2010; 618: 121-123.
http://dx.doi.org/10.1016/j.nima.2010.02.113

[147] Lattanzi D, Angelone M, Pillon M, Almaviva S, Marinellim, Milani E, Prestopino G, Tucciarone A, Verona C, Rinati G. Verona-, Popovichev S, Montereali RM, Vincenti MA, Murari A, and JET EFDA contributors. Single Crystal CVD Diamonds as Neutron Detectors at JET. Fusion Engineering and Design 2009; 84: 1156-1159.
http://dx.doi.org/10.1016/j.fusengdes.2008.12.005

[148] Angelone M, Pillon M, Marinelli Marco, Milani E, Prestopino G, Verona C, Rinati G. Verona-, Coffey I, Murari A, Tartoni N, JET-EFDA contributors. Single crystal artificial diamond detectors for VUV and soft X-rays measurements on JET thermonuclear fusion plasma. Nuclear Instruments and Methods in Physics Research A 2010; 623: 726-730.
http://dx.doi.org/10.1016/j.nima.2010.04.021

[149] Picollo F, Gatto Monticone D, Olivero P, Fairchild BA, Rubanov S, Prawer S, Vittone E. Fabrication and electrical characterization of three dimensional graphitic microchannels in single crystal diamond. New J Phys 2012; 14: 053011.
http://dx.doi.org/10.1088/1367-2630/14/5/053011

[150] Conte G, Allegrini P, Pacilli M, Salvatori S, Kononenko T, Bolshakov A, Ralchenko V, Konov V. Three-dimensional graphite electrode CVD single crystal diamond detectors: Charge collection dependence on impinging β-particles geometry. Nuclear Instruments and Methods in Physics Research A 2015; 799: 10-16.
http://dx.doi.org/10.1016/j.nima.2015.07.024

[151] Balling P, Esberg J, Kirsebom K, Le DQS, Uggerhøj UI, Connell SH, Härtwig J, Masiello F, Rommeveaux A. Bending diamonds by femtosecond laser ablation. Nuclear Instruments and Methods in Physics Research B 2009; 267: 2952-2957.
http://dx.doi.org/10.1016/j.nimb.2009.06.109

[152] Freund AK, Gsell S, Fischer M, Schreck M, Andersen KH, Courtois P, Borchert G, Skoulatos M. Diamond mosaic crystals for neutron instrumentation: First experimental results. Nuclear Instruments and Methods in Physics Research A 2011; 634: S28-S36.
http://dx.doi.org/10.1016/j.nima.2010.05.043

[153] Tsubouchi N, Mokuno Y, Kakimoto A, Konno Y, Yamada H, Chayahara A, Kaneko JH, Fujita F, Shikata S. Characterization of a sandwich-type large CVD single crystal diamond particle detector fabricated using a lift-off method. Diamond & Related Materials 2012; 24: 74-77.
http://dx.doi.org/10.1016/j.diamond.2011.11.003

[154] Motochi I, Naidoo SR, Mathe BA, Erasmus R, Aradi E, Derry TE, Olivier EJ. Surface Brillouin scattering on annealed ion-implanted CVD diamond. Diamond & Related Materials 2015; 56: 6-12.
http://dx.doi.org/10.1016/j.diamond.2015.03.022

[155] Almaviva S, Ciancaglioni I, Consorti R, Notaristefani F. De, Manfredotti C, Marinelli Marco, Milani E, Petrucci A, Prestopino G, Verona C, Rinati Verona G. Synthetic single crystal diamond dosimeters for conformal radiation therapy application. Diamond & Related Materials 2010: 19: 217-220.
http://dx.doi.org/10.1016/j.diamond.2009.10.007

[156] Almaviva S, Ciancaglioni I, Consorti R, Notaristefani F. De, Manfre-dotti C, Marinelli Marco, Milani E, Petrucci A, Prestopino G, Verona C, Rinati Verona G. Synthetic single crystal diamond dosimeters for Intensity Modulated Radiation Therapy applications. Nuclear Instruments and Methods in Physics Research 2009; A 608: 191-194.

[157] Tromson D, Pomorska M. Rebisz-, Tranchant N, Isambert A, Moignau F, Moussier A, Marczewska B, Bergonzo P. Single crystal CVD diamond detector for high resolution dose measurement for IMRT and novel radiation therapy needs. Diamond & Related Materials 2010; 19: 1012-1016.
http://dx.doi.org/10.1016/j.diamond.2010.03.008

[158] Schirru F, Kisielewicz K, Nowak T, Marczewska B. Single crystal diamond detector for radiotherapy. Journal of Physics D: Applied Physics, Institute of Physics: Hybrid Open Access 2010; 43 (26): 265101.
http://dx.doi.org/10.1088/0022-3727/43/26/265101

[159] Venanzio C. Di, Marinelli Marco, Milani E, Prestopino G, Verona C, and Rinatia G. Verona-, Falco M. D, Bagalà P, Santoni R, Pimpinella M. Characterization of a synthetic single crystal diamond Schottky diode for radiotherapy electron beam dosimetry. Med Phys 2013; 40: 021712-1- 021712-9.

[160] Ade N, Namn TL. The influence of detector size relative to field size in small-field photon-beam dosimetry using synthetic diamond crystals as sensors. Radiation Physics and Chemistry 2015; 113: 6-13.
http://dx.doi.org/10.1016/j.radphyschem.2015.04.005

[161] Ciancaglioni I, Marinelli Marco, Milani E, Prestopino G, Verona C, and G. Verona-Rinatia, Consorti R. and Petrucci A, Notaristefani F. De. Dosimetric characterization of a synthetic single crystal diamond detector in clinical radiation therapy small photon beams. Med Phys 2012; 39: 4493-4501.
http://dx.doi.org/10.1118/1.4729739

[162] Almaviva S, Marinelli Marco, Milani E, Prestopino G, Tucciarone A, Verona C, Rinati G. Verona, Angelone M, Pillon M. Extreme UV photodetectors based on CVD single crystal diamond in a p-type/intrinsic/metal configuration. Diamond & Related Materials 2009; 18: 101-105.
http://dx.doi.org/10.1016/j.diamond.2008.10.034

[163] Xiangyun C, Qiong W, Ilan B-Z, Andrew B, Jorg K, Triveni R, John S, Erdong W, Erik MM, Richard B, Dimitre Dv. Electron Beam Emission from a Diamond-Amplifier Cathode. PRL 2010; 105: 164801.
http://dx.doi.org/10.1103/PhysRevLett.105.164801

[164] Parkhomenko MP, Kalenov DS, Fedoseev NA, Eremin IS, Ralchenko VG, Bolshakov AP, Ashkinazi EE, Popovich AF, Balla VK, Mallik AK. Measurement of the Complex Permittivity of Polycrystalline Diamond by the Resonator Method in the Millimeter Range. Physics of Wave Phenomena 2015; 23: 1-6.
http://dx.doi.org/10.3103/S1541308X15030073

[165] Mallik AK, Pal KS, Dandapat N, Guha BK, Datta S, Basu D. Influence of The Microwave Plasma CVD Reactor Parameters on Substrate Thermal Management for Growing Large Area Diamond Coatings inside a 915 MHz and Moderately Low Power Unit. Diamond & Related Materials 2012; 30: 53-61.
http://dx.doi.org/10.1016/j.diamond.2012.10.001

[166] Mallik AK, Bysakh S, Pal KS, Dandapat N, Guha BK, Datta S, Basu D. Large area deposition of polycrystalline diamond coatings by microwave plasma CVD. Transactions of the Indian Ceramic Society 2013; 72: 225-232.
http://dx.doi.org/10.1080/0371750X.2013.870768

[167] Mallik AK, Bysakh S, Sreemany M, Roy S, Ghosh J, Roy S, Mendes JC, Gracio J, Datta S. Property mapping of polycrystalline diamond coatings over large area. Journal of Advanced Ceramics 2014; 3(1): 56-70.
http://dx.doi.org/10.1007/s40145-014-0093-1

[168] Yamada H, Meier A, Mazzocchi F, Schreck S, Scherer T. Dielectric properties of single crystalline diamond wafers with large area at microwave wavelengths. Diamond & Related Materials 2015; 58: 1-4.
http://dx.doi.org/10.1016/j.diamond.2015.05.004

[169] Tandon N, Albrecht JD, Mohan LR. Ram. Electron-phonon coupling and associated scattering rates in diamond. Diamond & Related Materials 2015; 56: 1-5.
http://dx.doi.org/10.1016/j.diamond.2015.03.019

[170] Kohn E, Adamschik M, Schmid P, Denisenko A, Aleksov A, Ebert W. Prospects of diamond devices. J Phys 2001; D 34: R77.

[171] Garino Y, Teraji T, Koizumi S, Koide Y, Ito T. p-type diamond Schottky diodes fabricated by vacuum ultraviolet light/ozone surface oxidation: Comparison with diodes based on wet-chemical oxidation. Phys Stat Sol 2009; (a) 206: 2082.

[172] Teraji T, Koide Y, Ito T. High-temperature stability of Au/p-type diamond Schottky diode. Phys Stat Sol (RRL) 2009; 3: 211.
http://dx.doi.org/10.1002/pssr.200903151

[173] Teraji T, Garino Y, Koide Y, Ito T. Low-leakage p-type diamond Schottky diodes prepared using vacuum ultraviolet light/ozone treatment. J Appl Phys 2009; 105: 126109.
http://dx.doi.org/10.1063/1.3153986

[174] Butler JE, Geis MW, Krohn KE, Lawless J, Deneault S, Lyszczarz TM, Flechtner D, Wright R. Exceptionally high voltage Schottky diamond diodes and low boron doping. Semicond Sci Technol 2003; 18: S67.
http://dx.doi.org/10.1088/0268-1242/18/3/309

[175] Aleksov A, Vescan A, Kunze M, Gluche P, Ebert W, Kohn E, Bergmaier A, Dollinger G. Diamond junction FETs based on δ-doped channels. Diamond Relat Mater 1999; 8: 941.
http://dx.doi.org/10.1016/S0925-9635(98)00393-8

[176] Vescan A, Daumiller I, Gluche P, Ebert W, Kohn E. High temperature, high voltage operation of diamond Schottky diode. Diamond Relat Mater 1998; 7: 581.
http://dx.doi.org/10.1016/S0925-9635(97)00200-8

[177] Vescan A, Ebert W, Borst T, Kohn E. IV characteristics of epitaxial Schottky Au barrier diode on p+ diamond substrate. Diamond Relat Mater 1995; 4: 661.
http://dx.doi.org/10.1016/0925-9635(94)05237-9

[178] Umezawa H, Ikeda K, Kumaresan R, Tatsumi N, Shikata S. Increase in reverse operation limit by barrier height control of diamond Schottky barrier diode. IEEE Electron Device Lett 2009; 30: 960.
http://dx.doi.org/10.1109/LED.2009.2026439

[179] Achard J, Silva F, Issaoui R, Brinza O, Tallaire A, Schneider H, Isoird K, Ding H, Koné S, Pinault MA, Jomard F, Gicquel A. Thick boron doped diamond single crystals for high power electronics. Diamond & Related Materials 2011; 20: 145-152.
http://dx.doi.org/10.1016/j.diamond.2010.11.014

[180] Umezawa H, Nagase M, Kato Y, Shikata S. High temperature application of diamond power device. High temperature application of diamond power device. Diamond & Related Materials 2012; 24: 201-205.
http://dx.doi.org/10.1016/j.diamond.2012.01.011

[181] Butler JE, Geis MW, Krohn KE, Lawless J, Deneault S, Lyszczarz TM, Flechtner D, Wright R. Exceptionally high voltage Schottky diamond diodes and low boron doping. Semicond Sci Technol 2003; 18: S67-S71.
http://dx.doi.org/10.1088/0268-1242/18/3/309

[182] Volpe PN, Muret P, Pernot J, Omnes F, Teraji T, Koide Y, Jomard F, Planson D, Brosselard P, Dheilly N, Vergne B, Scharnholz S. Extreme dielectric strength in boron doped homoepitaxial diamond. Appl Phys Lett 2010; 97.

[183] Twitchen DJ, White head AJ, Coe SE, Isberg J, Hammersberg J, Wikstrom T, Johansson E. High-voltage single-crystal diamond diodes. IEEE Trans. Electron Devices 2004; 51: 826-828.
http://dx.doi.org/10.1109/TED.2004.826867

[184] Umezawa H, Saito T, Tokuda N, Ogura M, Ri SG, Yoshikawa H, Shikata S. Leakage current analysis of diamond Schottky barrier diode. Appl Phys 2007; 90: 073506.
http://dx.doi.org/10.1063/1.2643374

[185] Kumaresan R, Umezawa H, Shikata S. Vertical structure Schottky barrier diode fabrication using insulating diamond substrate. Diamond Relat Mater 2010; 19: 1324-1329.
http://dx.doi.org/10.1016/j.diamond.2010.06.019

[186] Reinhard DK, Tran DT, Schuelke T, Becker MF, Grotjohn TA, Asmussen J. SiO2 antireflection layers for single-crystal diamond. Diamond & Related Materials 2012; 25: 84-86.
http://dx.doi.org/10.1016/j.diamond.2012.02.011

[187] Paci Jeffrey T, Belytschko T, Schatz GC. The mechanical properties of single-crystal and ultra-nanocrystalline diamond: A theoretical study. Chemical Physics 2005; 414: 351-358.

[188] Liang Q, Yan C-S, Meng Y, Lai J, Krasnicki S, Mao H-K, Hemley RJ. Enhancing the mechanical properties of single-crystal CVD diamond. J Phys Condens Matter 2009; 21: 364215 (6pp).

[189] Wang S, Meng Y-F, Ando N, Tate M, Krasnicki S, Yan C-S, Liang Q, Lai J, Mao H-K, Grunera SM, Hemley RJ. Single-crystal CVD diamonds as small-angle X-ray scattering windows for high-pressure research. J Appl Cryst 2012; 45: 453-457.
http://dx.doi.org/10.1107/S0021889812010722

[190] Christopher M. Breeding and James E. Shigley. The "Type" Classification System of Diamonds and its Importance in Gemology. Gems & Gemology 2009; 45: 96-111.
http://dx.doi.org/10.5741/GEMS.45.2.96

[191] Breeding Christopher M, Wang W. Occurrence of the Si-V defect center in natural colorless gem diamonds. Diamond & Related Materials 2008; 17: 1335-1344.
http://dx.doi.org/10.1016/j.diamond.2008.01.075

[192] Willems B, Tallaire A, Achard J. Optical study of defects in thick undoped CVD synthetic diamond layers. Diamond and Related Materials 2014; 41: 25-33.
http://dx.doi.org/10.1016/j.diamond.2013.09.010

[193] Blank E. Structural Imperfections in CVD, Diamond Films, Thin-Film Diamond I, edited by Christopher Nebel, Juergen Ristein, published by Elsevier Inc. 2003; Chapter 2: 49-144.

[194] Gainutdinov Radmir V, Shiryaev Andrey A, Boyko Vladimir S, Fedortchouk Yana. An Atomic Force Microscopy investigation. Diamond and Related Materials 2013; 40: 17-23.
http://dx.doi.org/10.1016/j.diamond.2013.09.006

[195] Yelisseyev AP, Vins VG, Lobanov SS, Afonin DV, Blinkov AE, Maximov AYu. Aggregation of donor nitrogen in irradiated Ni-containing synthetic diamonds. Journal of Crystal Growth 2011; 318: 539-544.
http://dx.doi.org/10.1016/j.jcrysgro.2010.10.043

[196] Jones R, Goss JP, Pintoc H, Palmer DW. Diffusion of nitrogen in diamond and the formation of A-centres. Diamond & Related Materials 2015; 53: 35-39.
http://dx.doi.org/10.1016/j.diamond.2015.01.002

[197] Kiefert L, Karampelas S. Use of the Raman spectrometer in gemmological laboratories: Review. Spectrochimica Acta 2011; A80: 119- 124.

[198] Martineau PM, Lawson SC, Taylor AJ, Quinn SJ, Evans DJF, Michael JC. Identification of Synthetic Diamond Grown Using Chemical Vapor Deposition (CVD). Gems & Gemology Spring 2004; 2-25.

[199] Wang W, Hall MS, Moe KS, Tower J, Moses TM. Latest-Generation CVD-Grown Synthetic Diamonds From Apollo Diamond Inc, Gems & Gemology, Winter 2007; 294-312.

[200] Wang W, Johansson UFS. D'Haenens, Johnson Paul, Moe Kyaw Soe, Emerson Erica, Newton Mark E, and Moses Thomas M. CVD Synthetic Diamonds From Gemesis Corp, Gems & Gemology, Summer 2012; 80-97.

[201] Johansson Ulrika F.S. D'Haenens, Moe Kyaw Soe, Johnson Paul, Wong Shun Yan, Lu Ren, and Wang Wuyi. Near-Colorless HPHT Synthetic Diamonds from AOTC Group, Gems & Gemology, Spring. 2014; 50: no. 1.

[202] Choudhary D, Bellare J. Manufacture of gem quality diamonds: a review. Ceramics International 2000; 26: 73-85.
http://dx.doi.org/10.1016/S0272-8842(99)00022-X

[203] Burns RC, Hansen JO, Spits RA, Sibanda, Welbourn MCM, Welch DL. Growth of high purity large synthetic diamond crystals. Diamond and Related Materials 1999; 8: 1433-1437.
http://dx.doi.org/10.1016/S0925-9635(99)00042-4

[204] Sumiya H, Satoh S. High-pressure synthesis of high-purity diamond crystal. Diamond and Related Materials 1996; 5: 1359-1365.
http://dx.doi.org/10.1016/0925-9635(96)00559-6

[205] Sumiya H, Toda N, Satoh S. Growth rate of high-quality large diamond crystals. Journal of Crystal Growth 2002; 237-239: 1281-1285.
http://dx.doi.org/10.1016/S0022-0248(01)02145-5

[206] Cartigny P, Palot M, Thomassot E, Harris JW. Diamond Formation: A Stable Isotope Perspective, Review in Advance, first posted online on April 3, 2014; 699-732.

[207] Magaña SE. Comparison of luminescence lifetimes from natural and laboratory irradiated diamonds. Diamond & Related Materials 2015; 58: 94-102.
http://dx.doi.org/10.1016/j.diamond.2015.06.007

[208] Neu E, Steinmetz D, Riedrich-Moller J, Gsell S, Fischer M, Schreck M, Becher C. Single photon emission from silicon-vacancy colour centres in chemical vapour deposition nano-diamonds on iridium. New Journal of Physics 2011; 13: 025012.
http://dx.doi.org/10.1088/1367-2630/13/2/025012

[209] Neu E, Fischer M, Gsell S, Schreck M, Becher C, Fluorescence and polarization spectroscopy of single silicon vacancy centers in heteroepitaxial nanodiamonds on iridium. New Journal of Physics 2011; 84: 205211.
http://dx.doi.org/10.1103/physrevb.84.205211

[210] Loubser J, Wyk JA. van. Electron spin resonance in the study of diamond. Reports on Progress in Physics 1978; 41: 1201.
http://dx.doi.org/10.1088/0034-4885/41/8/002

[211] Reddy NRS, Manson NB, Krausz ER. Two-laser spectral hole burning in a colour centre in diamond. Journal of Luminescence 1987; 38: 46.
http://dx.doi.org/10.1016/0022-2313(87)90057-3

[212] Oort E. van, Manson NB, Glasbeek M. Optically detected spin coherence of the diamond NV centre in its triplet ground state. Journal of Physics C-Solid State Physics 1988; 21: 4385.
http://dx.doi.org/10.1088/0022-3719/21/23/020

[213] Davies G, Hamer MF. Optical Studies of the 1.945 eV Vibronic Band in Diamond. Proceedings of the Royal Society of London Series a-Mathematical Physical and Engineering Sciences 1976; 348: 285.
http://dx.doi.org/10.1098/rspa.1976.0039

[214] Khan RUA, Cann BL, Martineau PM, Samartseva J, Freeth JJP, Sibley SJ, Hartland CB, Newton ME, Dhillon HK, Twitchen DJ. Colour-causing defects and their related optoelectronic transitions in single crystal CVD diamond. Journal of Physics: Condensed Matter 2013; 25: 275801.
http://dx.doi.org/10.1088/0953-8984/25/27/275801

[215] Itoh Kohei M, Watanabe H. Isotope engineering of silicon and diamond for quantum computing and sensing applications. MRS Communications 2014; 4: 143-157.
http://dx.doi.org/10.1557/mrc.2014.32

[216] Balasubramanian G, Neumann P, Twitchen D, Markham M, Kolesov R, Mizuochi N, Isoya J, Achard J, Beck J, Tissler J, Jacques V, Hemmer PR, Jelezko F, Wrachtrup J. Ultralong spin coherence time in isotopically engineered diamond. Nat Mater 2009; 8: 383-387.
http://dx.doi.org/10.1038/nmat2420

[217] Maurer PC, Maze JR, Stanwix PL, Jiang L, Gorshkov AV, Zibrov AA, Harke B, Hodges JS, Zibrov AS, Yacoby A, Twitchen D, Hell SW, Walsworth RL, Lukin MD. Far-field optical imaging and manipulation of individual spins with nanoscale resolution. Nature Physics 2010; 6: 912-918.
http://dx.doi.org/10.1038/nphys1774

[218] Gruber A, Drabenstedt A, Tietz C, Fleury L, Wrachtrup J, Borczyskowski C. Von. Scanning Confocal Optical Microscopy and Magnetic Resonance on Single Defect Centers. Science 1997; 276: 2012-2014.
http://dx.doi.org/10.1126/science.276.5321.2012

[219] Edmonds AM. Magnetic resonance studies of point defects in single crystal diamond, PhD Thesis, University of Warwick, Department of Physics, 2008.

[220] Sum Wilson Chin Yue. Towards magnetometry with nitrogen-vacancy center in diamond, Undergraduate Thesis, Department of Physics, National University of Singapore, 2012/2013.

[221] Schwartz J, Aloni S, Ogletree DF, Schenkel T. Effects of low energy electron irradiation on formation of nitrogen-vacancy centers in single-crystal diamond. New J Phys 2012; 14: 043024.
http://dx.doi.org/10.1088/1367-2630/14/4/043024

[222] Schirhagl R, Chang K, Loretz M, Degen CL. Nitrogen-Vacancy Centers in Diamond: Nanoscale Sensors for Physics and Biology. Annu Rev Phys Chem 2014; 65: 83-105.
http://dx.doi.org/10.1146/annurev-physchem-040513-103659

[223] Waldermann FC, Olivero P, Nunn J, Surmacz K, Wang ZY, Jaksch D, Taylor RA, Walmsley IA, Draganski M, Reichart P, Greentree AD, Jamieson DN, Prawer S. Creating diamond color centers for quantum optical applications. Diamond & Related Materials 2007; 16: 1887-1895.
http://dx.doi.org/10.1016/j.diamond.2007.09.009

[224] Tallaire A, Lesik M, Jacques V, Pezzagna S., Mille V, Brinza O, Meijer J, Abel B, Roch JF, Gicquel A, Achard J. Temperature dependent creation of nitrogen-vacancy centers in single crystal CVD diamond layers. Diamond & Related Materials 2015; 51: 55-60.
http://dx.doi.org/10.1016/j.diamond.2014.11.010

[225] Manson NB, Harrison JP. Photo-ionization of the nitrogen-vacancy center in diamond. Diamond & Related Materials 2005; 14: 1705-1710.
http://dx.doi.org/10.1016/j.diamond.2005.06.027

[226] Kim M, Mamin HJ, Sherwood MH, Ohno K, Awschalom DD, Rugar D. Decoherence of near-surface nitrogen-vacancy centers due to electric field noise. Phys Rev Lett 2015; 115: 087602.
http://dx.doi.org/10.1103/PhysRevLett.115.087602

[227] Toyli David M, Weis Christoph D, Fuchs Gregory D, Schenkel Thomas, Awschalom David D. Chip-Scale Nanofabrication of Single Spins and Spin Arrays in Diamond. Nano Lett 2010; 10: 3168-3172.
http://dx.doi.org/10.1021/nl102066q

[228] Schwartz J, Michaelides P, Weis C D, Schenkel T. In situ optimization of co-implantation and substrate temperature conditions for nitrogen-vacancy center formation in single-crystal diamonds. New Journal of Physics 2011; 13: 035022.
http://dx.doi.org/10.1088/1367-2630/13/3/035022

[229] Latawie P, Venkataraman V, Burek MJ, Hausmann BJM, Bulu I, Lončar M. On-Chip Diamond Raman Laser 2015; arXiv-150900373.

[230] Mildren RP, Butler JE, Rabeau JR. CVD-diamond external cavity Raman laser at 573 nm. Opt Express 2008; 16: 18950-18955.
http://dx.doi.org/10.1364/OE.16.018950

[231] Mildren RP, Sabella A. Highly efficient diamond Raman laser. Opt Lett 2009; 34: 2811-2813.
http://dx.doi.org/10.1364/OL.34.002811

[232] Lubeigt W, Bonner GM, Hastie JE, Dawson MD, Burns D, Kemp AJ. An intra-cavity Raman laser using synthetic single-crystal diamond. Opt Express 2010; 18: 16765-16770.
http://dx.doi.org/10.1364/OE.18.016765

[233] Sabella A, Piper JA, Mildren RP. 1240 nm diamond Raman laser operating near the quantum limit. Opt Lett 2010; 35: 3874-3876.
http://dx.doi.org/10.1364/OL.35.003874

[234] Spence DJ, Granados E, Mildren RP. Mode-locked picoseconds diamond Raman laser. Opt Lett 2010; 35: 556-558.
http://dx.doi.org/10.1364/OL.35.000556

[235] Doherty Marcus W, Manson Neil B, Delaney Paul, Jelezko Fedor, Wrachtrup Jörg, Hollenberg Lloyd CL. The nitrogen-vacancy colour centre in diamond. Physics Reports 2013; 528(1): 1-45.

[236] Acosta VM. Optical Magnetometry with Nitrogen-Vacancy Centers in Diamond, PhD Thesis, Physics in the Graduate Division of the University of California, Berkeley, 2011.

[237] Balasubramanian G, Chan IY, Kolesov R, Hmoud M. Tisler Al-, J, Shin C, Kim C, Wojcik A, Hemmer PR, Krueger A, Hanke T, Leitenstorfer A, Bratschitsch R, Jelezko F, Wrachtrup J. Nanoscale imaging magnetometry with diamond spins under ambient conditions. Nature 455: 648-651.

[238] Maze JR, Stanwix PL, Hodges JS, Hong S, Taylor JM, Cappellaro P, Jiang L, Dutt MVG, Togan E, Zibrov AS, Yacoby A, Walsworth RL, Lukin MD. Nanoscale magnetic sensing with an individual electronic spin in diamond. Nature 2008; 455: 644.
http://dx.doi.org/10.1038/nature07279

[239] Maze JR, Stanwix PL, Hodges JS, Hong S, Taylor JM, Cappellaro P, Jiang L, Dutt MV, Gurudev, Togan E, Zibrov AS, Yacoby A, Walsworth RL, Lukin MD. Nanoscale magnetic sensing with an individual electronic spin in diamond. Nature 2008; 455: 644.
http://dx.doi.org/10.1038/nature07279

[240] Dolde F, Fedder H, Doherty MW, Nöbauer T, Rempp F, Balasubramanian G, Wolf T, Reinhard F, Hollenberg LCL, Jelezko F, Wrachtrup J. Electric-field sensing using single diamond spins. Nature Phys 2011; 7: 459.
http://dx.doi.org/10.1038/nphys1969

[241] Bassett LC, Heremans FJ, Yale CG, Buckley BB, Awschalom DD. Electrical Tuning of Single Nitrogen-Vacancy Center Optical Transitions Enhanced by Photoinduced Fields. Physical Review Letters 2011; 107: 266403.
http://dx.doi.org/10.1103/PhysRevLett.107.266403

[242] Kucsko G, Maurer PC, Yao NY, Kubo M, Noh HJ, Lo PK, Park H, Lukin MD. Nanometre-scale thermometry in a living cell. Nature 2013; 500: 54-58.
http://dx.doi.org/10.1038/nature12373

[243] Ovartchaiyapong P, Lee KW, Myers BA, Jayich AC. Bleszynski. Dynamic strain-mediated coupling of a single diamond spin to a mechanical resonator. Nature Communications 2014; 5: 4429.

[244] DeVience Stephen J, Pham Linh M, Lovchinsky Igor, Sushkov Alexander O, Bar-Gill Nir, Belthangady Chinmay, Casola Francesco, Corbett Madeleine, Zhang Huiliang, Lukin Mikhail, Park Hongkun, Yacoby Amir, Walsworth Ronald L, Nanoscale NMR spectroscopy and imaging of multiple nuclear species. Nature Nanotechnology 2015; 10: 129-134.

[245] Drezeta A, Sonnefrauda Y, Cuchea A, Molleta O, Berthela M, Huanta S. Near-field microscopy with a scanning nitrogen-vacancy color center in a diamond nanocrystal: A brief review, Micron 2015; 70: 55-63.
http://dx.doi.org/10.1016/j.micron.2014.12.004

[246] Sushkov AO, Lovchinsky I, Chisholm N, Walsworth RL, Park H, Lukin MD. Magnetic Resonance Detection of Individual Proton Spins Using Quantum Reporters. Phys Rev Lett 2014; 113: 197601.
http://dx.doi.org/10.1103/PhysRevLett.113.197601

[247] Iv´ady V, Sz´asz K, Falk AL, Klimov PV, Christle DJ, Janz´en E, Abrikosov IA, Awschalom DD, Gali A. Theoretical model of the dynamic spin polarization of nuclei coupled to paramagnetic point defects in diamond and silicon carbide. Phys Rev 2015; B92: 115206.

[248] Auer A, Burkard G, Long-range photon-mediated gate scheme between nuclear spin qubits in diamond, 2015; arXiv:1507,08468.

[249] Dutt MV Gurudev, Childress L, Jiang L, Togan E, Maze J, Jelezko F, Zibrov AS, Hemmer PR, Lukin MD. Quantum Register Based on Individual Electronic and Nuclear Spin Qubits in Diamond. Science 2007; 316: 1312.
http://dx.doi.org/10.1126/science.1139831

[250] Wolf SA, Rosenberg I, Rapaport R, Bar-Gill N. Purcell-enhanced optical spin readout of Nitrogen-Vacancy centers in diamond 2015; arXiv:1505.01006.

[251] Janitz E, Ruf M, Dimock M, Bourassa A, Sankey J, Lilian C. A Fabry-Perot Microcavity for Diamond-Based Photonics 2015; arXiv:1508.06588.

[252] Faraon A, Santori C, Huang Z, Fu K-MC, Acosta VM, David F, Beausoleil RG. Quantum photonic devices in single-crystal diamond. New Journal of Physics 2013; 15: 025010.

[253] Aharonovich I, Greentree AD, Prawer S. Diamond Photonics. Nature Photonics 2011; 5: 397-405.
http://dx.doi.org/10.1038/nphoton.2011.54

[254] Chu Y, Leon NP. de, Shields BJ, Hausmann B, Evans R, Togan E, Burek MJ, Markham M, Stacey A, Zibrov AS, Yacoby A, Twitchen DJ, Loncar M, Park H, Maletinsky P, Lukin MD. Coherent Optical Transitions in Implanted Nitrogen Vacancy Centers. Nano Letters 2014; 14: 1982.
http://dx.doi.org/10.1021/nl404836p

[255] Mouradian SL, Oder T. Schr, Poitras CB, Li L, Goldstein J, Chen EH, Walsh M, Cardenas J, Markham ML, Twitchen DJ, Lipson M, Englund D. Scalable Integration of Long-Lived Quantum Memories into a Photonic Circuit. Phys Rev X 2015; 5: 031009.
http://dx.doi.org/10.1103/PhysRevX.5.031009

[256] M Hausmann BJ, Shields BJ, Quan Q, Chu Y, Leon NP. de, Evans R, Burek MJ, Zibrov AS, Markham M, Twitchen DJ, Park H, Lukin MD, Lončar M. Coupling of NV centers to photonic crystal nanobeams in diamond. Nano Lett 2013; 13: 5791.
http://dx.doi.org/10.1021/nl402174g

[257] Burek Michael J, Leon Nathalie P. de, Shields Brendan J, Hausmann Birgit JM, Yiwen Chu, Quan Qimin, Zibrov Alexander S, Park Hongkun, Lukin Mikhail D, Lončar Marko. Free-standing mechanical and photonic nanostructures in single-crystal diamond. Nano Lett 2012; 12: 6084.
http://dx.doi.org/10.1021/nl302541e

[258] Chu Y, Leon NP. de, Shields BJ, Hausmann B, Evans R, Togan E, Burek MJ, Stacey Markham M, Zibrov AS, Yacoby A, Twitchen DJ, Loncar M, Park H, Maletinsky P, Lukin MD. Coherent optical transitions in implanted nitrogen vacancy centers. Nano Lett 2014; 14: 1982.
http://dx.doi.org/10.1021/nl404836p

[259] Burek Michael J, Chu Yiwen, Liddy Madelaine SZ, Patel Parth, Rochman Jake, Meesala Srujan, Hong Wooyoung, Quan Qimin, Lukin Mikhail D, Lončar Marko. High quality-factor optical nanocavities in bulk single-crystal diamond. Nat Commun 2014; 5: 5718.

[260] Mizuochi N, Makino T, Kato H, Takeuchi D, Ogura M, Okushi H, Nothaft M, Neumann P, Gali A, Jelezko F, Wrachtrup J, Yamasaki S. Electrically driven single-photon source at room temperature in diamond. Nature Photon 2012; 6: 299.
http://dx.doi.org/10.1038/nphoton.2012.75

[261] Lohrmann A, Pezzagna S, Dobrinets I, Spinicelli P, Jacques V, Roch J-F, Meijer J, Zaitsev AM. Diamond based light-emitting diode for visible single-photon emission at room temperature. Appl Phys Lett 2011; 99: 251106.
http://dx.doi.org/10.1063/1.3670332

[262] Hausmann Birgit JM, Khan M, Zhang Y, Babinec TM, Martinickc K, McCutcheon M, Hemmer PR, Loncar M. Fabrication of Diamond Nanowires for Quantum Information Processing Applications. Diamond & Related Materials 2010; 19: 621-629.
http://dx.doi.org/10.1016/j.diamond.2010.01.011

[263] Burek Michael J, Leon Nathalie P. de, Shields Brendan J, Hausmann Birgit JM, Chu Yiwen, Quan Qimin, Zibrov Alexander S, Park Hongkun, Lukin Mikhail D, Lončar Marko. Free-Standing Mechanical and Photonic Nanostructures in Single- Crystal Diamond. Nano Lett 2012; 12: 6084−6089.
http://dx.doi.org/10.1021/nl302541e

[264] Zalalutdinov MK, Baldwin JW, Pate BB, Yang J, Butler JE, Houston BH. Single Crystal Diamond Nanomechanical Dome Resonator. NRL Review 2008; 190-191.

[265] Liao, Meiyong, Hishita, Shunichi, Koide, Yasuo, & Li, Chun (2010). Batch production of single-crystal diamond bridges and cantilevers for microelectromechanical systems. Journal of Micromechanics and Microengineering Structures, Devices and Systems, 20(8), 6.
http://dx.doi.org/10.101088/0960-1317/20/8/085002

[266] Liao M, Hishita S, Watanabe E, Koizumi S, Koide Y. Suspended Diamond Nanowires for High-Performance Nanoelectromechanical Switches Single-Crystal. Adv Mater 2010; 22: 5393-5397.
http://dx.doi.org/10.1002/adma.201003074

[267] Burek MJ, Chu Y, Liddy MSZ, Patel P, Rochman J, Meesala S, Hong W, Quan Q, Lukin MD, Lončar M. High quality-factor optical nanocavities in bulk single-crystal diamond. Nature Communications 2014; 5: 5718.
http://dx.doi.org/10.1038/ncomms6718

[268] Lin Z, Johnson SG, Rodriguez AW, Loncar M. Design of diamond microcavities for single photon frequency down-conversion. Opt Express 2015; 23: 25279.
http://dx.doi.org/10.1364/OE.23.025279

[269] Burek MJ, Chu Y, Liddy MSZ, Patel P, Rochman J, Meesala S, Hong W, Quan Q, Lukin MD, Lončar M. High-Q Optical Nanocavities in Bulk Single-Crystal Diamond. Nature Communications 2014; 5: 5718.
http://dx.doi.org/10.1038/ncomms6718

[270] Checoury X, Neel D, Boucaud P, Gesset C, Girard H, Saada S, Bergonzo P. Nanocrystalline diamond photonics platform with high quality factor photonic crystal cavities. Appl Phys Lett 2012; 101: 171115.
http://dx.doi.org/10.1063/1.4764548

[271] Wolters J, Schell AW, Kewes G, Nusse N, Schoengen M, Doscher H, Hannappel T, Lochel B, Barth M, Benson O. Enhancement of the zero phonon line emission from a single NV- center in a nanodiamond via coupling to a photonic crystal cavity. Applied Physics Letters 2010; 97: 141108.
http://dx.doi.org/10.1063/1.3499300

[272] Moller JR, Kipfstuhl L, Hepp C, Neu E, Pauly C, Mu¨cklich F, Baur A, Wandt M, Wolff S, Fischer M, Gsell S, Schreck M, Becher C. One- and two-dimensional photonic crystal microcavities in single crystal diamond. Nature Nanotechnology 2012; 7: 69-74.
http://dx.doi.org/10.1038/nnano.2011.190

[273] Ureña EB, Ballestero CG, Geiselmann M, Marty R, Radko IP, Holmgaard T, Alaverdyan Y, Moreno E, García-Vidal FJ, Bozhevolnyi SI, Quidant R. Coupling of individual quantum emitters to channel plasmons. Nature Commun 2015; 6: 7883.
http://dx.doi.org/10.1038/ncomms8883

[274] Dibos A. Nanofabrication of Hybrid Optoelectronic Devices, Doctoral dissertation Harvard University. Graduate School of Arts & Sciences 2015.

[275] Bayn I, Mouradian S, Li L, Goldstein JA, Schröder T, Zheng J, Chen EH, Gaathon O, Lu M, Stein A, Ruggiero CA, Salzman J, Kalish R, Englund D. Fabrication of Triangular Nanobeam Waveguide Networks in Bulk Diamond Using Single-Crystal Silicon Hard Masks. Appl Phys Lett 2014; 105: 211101.
http://dx.doi.org/10.1063/1.4902562

[276] Khanaliloo B, Jayakumar H, Lake DP, Barclay PE. Diamond nanobeam waveguide optomechanics, CLEO: Science and Innovations. Optical Society of America 2015; paper STh3I.3.
http://dx.doi.org/10.1364/CLEO_SI.2015.STh3I.3

[277] Obraztsov AN, Kopylov PG, Loginov BA, Dolganov MA, Ismagilov RR, Savenko NV. Single crystal diamond tips for scanning probe microscopy. Review of Scientific Instruments 2010; 81: 013703.
http://dx.doi.org/10.1063/1.3280182

[278] Zolotukhin AA, Dolganov MA, Alekseev AM, Obraztsov AN. Single-crystal diamond microneedles shaped at growth stage. Diamond & Related Materials 2014; 42: 15-20.
http://dx.doi.org/10.1016/j.diamond.2013.09.00

[279] Odake S, Ohfuji H, Okuchi T, Kagi H, Sumiya H, Irifune T. Pulsed laser processing of nano-polycrystalline diamond: A comparative study with single crystal diamond. Diamond & Related Materials 2009; 18: 877-880.
http://dx.doi.org/10.1016/j.diamond.2008.10.066

[280] Heremans FJ, Fuchs GD, Wang CF, Hanson R, Awschalom DD. Generation and transport of photoexcited electrons in single-crystal Diamond. Applied Physics 2009; 94: 152102.
http://dx.doi.org/10.1063/1.3120225

[281] Neu E, Hepp C, Hauschild M, Gsell S, Fischer M, Sternschulte H, Uller-Nethl DS, Schreck M, Becher C. Low-temperature investigations of single silicon vacancy colour centres in diamond. New Journal of Physics 2013; 15: 043005.
http://dx.doi.org/10.1088/1367-2630/15/4/043005

[282] Sedov V, Ralchenko V, Khomich AA, Vlasov I, Vul A, Savind S, Goryacheve A, Konov V. Si-doped nano- and microcrystalline diamond films with controlled bright photoluminescence of silicon-vacancy color centers. Diamond & Related Materials 2015; 56: 23-28.
http://dx.doi.org/10.1016/j.diamond.2015.04.003

[283] Zhang JL, Ishiwata H, Babinec TM, Radulaski M, Müller K, Lagoudakis KG, Dahl J, Edgington R, Soulière V, Gabriel F, Fokin AA, Schreiner PR, Shen Z-X, Melosh NA, Vučković J. Hybrid Group IV Nanophotonic Structures Incorporating Diamond Silicon-Vacancy Color Centers, Nano Lett 2016; 16: 212-217.
http://dx.doi.org/10.1021/acs.nanolett.5b03515

[284] Lee JC, Aharonovich I, Magyar AP, Rol F, Hu EL. Coupling of silicon-vacancy centers to a single crystal diamond cavity. Optics Express 2012; 20: 8891.

[285] "Diamond quantum computers using NV- centres" on YouTube. https://youtu.be/WtzNCTCSQY0, last accessed on 16th October, 2015.

[286] "Diamonds are a quantum computer's best friends" on YouTube. https://youtu.be/vacbk1b7IEc, last accessed on 16th October, 2015.